LASER BIOSTIMULATION AND MONITORIZATION OF WOUND HEALING BY MEANS OF BIOIMPEDANCE MEASUREMENTS

by

Hakan Solmaz

B.Sc., Physics, Boğaziçi University, 2005

M.Sc., Institute of Biomedical Engineering, Boğaziçi University, 2008

Submitted to the Institute of Biomedical Engineering

in partial fulfillment of the requirements

for the degree of

Doctor

of

Philosophy

Boğaziçi University

2016

To my family...

ACKNOWLEDGMENTS

I would like to express my special thanks to my thesis advisor, Prof. Dr. Yekta Ülgen, for his guidance and valuable criticism throughout my study.

I am greatful to my thesis co-advisor Prof. Dr. Murat Gülsoy for his endless help and support during this study.

I would like to thank Assoc. Prof. Dr. Bora Garipcan for his support and for giving me the opportunity to use all of the facilities of Biomaterials Laboratory during my research.

I would like to thank my friends for their support and patience during my study.

I would like to thank my family for their support and belief for my thesis.

I am very specially thankful to my wife Edona Lacin Solmaz for her support and encouragement during my work.

My dear son, Ron Kaan Solmaz, I am so lucky that you are my son.

ACADEMIC ETHICS AND INTEGRITY STATEMENT

I, Hakan Solmaz, hereby certify that I am aware of the Academic Ethics and Integrity Policy issued by the Council of Higher Education (YÖK) and I fully acknowledge all the consequences due to its violation by plagiarism or any other way.

Name :

Signature:

Date:

ABSTRACT

LASER BIOSTIMULATION AND MONITORIZATION OF WOUND HEALING BY MEANS OF BIOIMPEDANCE MEASUREMENTS

Wound healing is critically important for the quality of life. Substantial number of patients suffering from non-healing chronic wounds and having serious difficulties in their daily life are reported in wound healing studies. However the exact mechanism of healing is not fully understood yet. Scientists have been investigating modalities for stimulating the wound healing process. Laser photobiomodulation has become widespread supporting the idea of therapeutic effects of laser irradiation in biological tissues recently. Conventional methods for following the healing generally lack of objectiveness and repeatability. Thus, a new non-invasive, repeatable and cost effective method was needed.

The aim of this study was to investigate the laser photobiomodulation on wound healing and monitor the healing process in-vivo by means of multi-frequency electrical bioimpedance measurements. Photobiomodulated in-vitro cell proliferation examinations were followed by in-vivo experiments on cutaneous skin wounds. Changes in the electrical properties of the wounds were examined with multi-frequency electrical impedance measurements on predetermined days of healing. Morphological, histological and mechanical examinations were used to find out the relationship between electrical properties of tissues and cellular events occurring during the healing process. Our findings showed the biostimulating effects of laser irradiation both in-vitro and in-vivo. The electrical impedance measurement results supported the idea of laser biostimulation on healing of cutaneous skin wounds. It is also shown that electrical bioimpedance measurements may be considered as a supporting non-invasive method for monitoring the healing process of skin wounds.

Keywords: Photobiomodulation (PBM), Laser Biostimulation, Wound Healing, Bioimpedance Measurements, Tensile Strength, Therapeutic.

ÖZET

LASER BİYOUYARIM İLE YARA İYİLEŞMESİNİN HIZLANDIRILMASI VE İYİLEŞMENİN BİYOEMPEDANS ÖLÇÜMLERİYLE GÖRÜNTÜLENMESİ

Yara iyileşmesi canlıların yaşam kalitesi üzerinde oldukça önemli bir etkendir. İyileşmeyen kronik yaralar nedeniyle günlük yaşamında ciddi engellerle karşılaşan hastalar ile ilgili çok sayıda çalışma vardır. Ancak, iyileşmenin mekanizmaısı henüz tam olarak anlaşılamamış olup iyileşmenin hızlandırılmasına yönelik araştırmalar devam etmektedir. İyileşme üzerinde olumlu yönde etkilerinin olduğu pek çok çalışmada gösterilmiş olan laser fotobiyomodülasyon araştırmalarına olan ilgi gün geçtikçe artmaktadır. Günümüzde yara iyileşmesi takibinde kullanılan geleneksel yöntemler genellikle taraflı ve tekrarlanabilirliği güç metodlardır. Bu nedenle girişimsel olmayan, nesnel, tekrarlanılabilir ve uygun fiyatlı bir yönteme ihtiyaç vardır.

Bu çalışmanın amacı laser fotobiyomodülasyonun yara iyileşmesi üzerindeki etkilerinin incelenmesi ve iyileşme sürecinin girişimsel olmayan çoklu-frekans elektriksel biyoempedans ölçümleri ile takip edilmesidir. Bu amaçla, laser fotobiyomodülasyonun öncelikle hücre kültürlerinin çoğalması, sonrasında cilt yaralarının iyileşmesi üzerindeki etkileri incelenmiştir. İyileşmenin belirli günlerinde alınan çoklu-frekans biyoempedans ölçümleri ile dokuların elektriksel özelliklerindeki değişimler elde edilmiştir. Yara örnekleri üzerinde yapılan biçimsel, histolojik ve mekanik değerlendirmelerin sonuçları ile elektriksel biyoempedans ölçümlerinin sonuçları karşılıklı değerlendirilmiştir. Elde edilen sonuçlar ile laser fotobiyomodülasyonun yüzeysel cilt yaralarının iyileşme süreçleri üzerindeki olumlu etkileri gösterilmiştir. Ayrıca, elde edilen sonuçlar çerçevesinde elektriksel biyoempedans ölçümlerinin iyileşmenin takibinde kullanılabilecek destekleyici bir yöntem olabileceği sonucuna ulaşılmıştır.

Anahtar Sözcükler: Fotobiyomodülasyon, Laser Biyo-uyarım, Yara İyileşmesi, Biyoempedans Ölçümleri, Kopma Direnci, İyileştirici.

TABLE OF CONTENTS

ACKNOWLEDGMENTS iv
ACADEMIC ETHICS AND INTEGRITY STATEMENT v
ABSTRACT vi
ÖZET vii
LIST OF FIGURES xi
LIST OF TABLES xv
LIST OF SYMBOLS xvi
LIST OF ABBREVIATIONS xvii
1. INTRODUCTION 1
1.1 Motivation 1
1.2 Objectives 2
1.3 Outline 3
2. BACKGROUND 4
2.1 WOUND HEALING 4
2.1.1 PHASES OF WOUND HEALING 4
2.1.1.1 Hemostasis 4
2.1.1.2 Inflammation 6
2.1.1.3 Proliferation 7
2.1.1.4 Maturation 10
2.1.2 WOUND TYPES 11
2.1.3 THE SKIN 13
2.1.3.1 The Epidermis 13
2.1.3.2 The Dermis 14
2.1.3.3 Subcutaneous Tissue 14
2.1.4 Optical Properties of Skin 15
2.2 PHOTOBIOMODULATION 16
2.3 ELECTRICAL IMPEDANCE 18
2.3.1 BIOIMPEDANCE MEASUREMENTS 19
2.3.2 COLE-COLE PLOT REPRESENTATION 22

3. MATERIALS AND METHODS 24
3.1 EXPERIMENTAL DESIGN OF THE STUDY 24
3.2 IN-VITRO CELL VIABILITY 24
3.2.1 CELL PREPERATION 24
3.2.2 MTT ANALYSIS 25
3.3 IN-VIVO WOUND EXPERIMENTS 25
3.3.1 ANIMAL PREPERATION 25
3.3.2 SURGERIES 26
3.3.3 POST SURGERY 27
3.4 PHOTOBIOMODULATION EXPERIMENTS 27
3.4.1 LASER IRRADIATION 27
3.4.2 LASER SAFETY 28
3.5 TENSILE STRENGTH MEASUREMENTS 28
3.6 BIOELECTRICAL IMPEDANCE MEASUREMENTS 29
3.7 HISTOLOGICAL EXAMINATIONS 31
3.7.1 TISSUE PROCESSING 31
3.7.2 PARAFFIN EMBEDDING 32
3.7.3 TISSUE SECTIONING 32
3.7.4 TISSUE STAINING 33
3.7.5 HISTOLOGICAL EVALUATION 34
3.8 STATISTICAL ANALYSIS 34
4. RESULTS AND DISCUSSION 35
4.1 IN-VITRO CELL VIABILITY 35
4.1.1 635 nm LASER IRRADIATION 36
4.1.2 809 nm LASER IRRADIATION 37
4.2 TENSILE STRENGTH 39
4.2.1 635 nm LASER IRRADIATION 39
4.2.2 809 nm LASER IRRADIATION 40
4.3 BIOELECTRICAL IMPEDANCE 41
4.3.1 BIOIMPEDANCE MEASUREMENTS 41
4.3.2 COLE-COLE PLOTS 44
4.4 HISTOLOGICAL EVALUATIONS 47

4.4.1 INCISIONAL WOUNDS 47
4.4.2 EXCISIONAL WOUNDS 48
4.4.2.1 Semi-quantitative Evaluations 49
5. DISCUSSIONS AND CONCLUSSION 54
REFERENCES 61

LIST OF FIGURES

Figure 2.1	Events occurring during acute wound healing. The complex structure shows the interdependency of various events from the beginning to the final phases of healing. Cytokines play a central role in wound healing and serve as a central signal for various cell types and healing events [31].	5
Figure 2.2	The complex relationship between various cell types and inflammatory markers during acute wound healing [31].	6
Figure 2.3	Schematic of the complex cellular and subcellular interactions of wound healing with the major participants, from inflammation to maturation [27].	11
Figure 2.4	Varying thickness of Stratum Corneum [62].	14
Figure 2.5	Penetration depth of light at various wavelengths through healthy skin [11].	17
Figure 2.6	Graphical representation of the complex impedance.	18
Figure 2.7	Three element equivalent models of a single cell in series and parallel combinations. In the first series combination model, Cs and Rs refer to the conductance created by the sweat ducts and resistance due to the outermost layer of the skin (stratum corneum). Rd in series represents the resistance of deeper layers. In the parallel combination model, Cm is the membrane capacitance, whereas Ri and Re are the resistances of intracellular and extracellular fluids respectively [79].	19
Figure 2.8	Frequency dependent response of biological tissues against an applied alternating current.	20
Figure 2.9	Electrically equivalent circuit model of a single cell.	21
Figure 2.10	Cole-Cole plot diagram gives the frequency dependent relationship between the real (Resistance) and imaginary (Reactance) parts of the complex electrical impedance of biological tissues.	23

Figure 3.1	Experimental design of the study. In-vitro cell viability experiments were followed by in-vivo wound photobiomodulation experiments.	24
Figure 3.2	Incisional and excisional wound models.	26
Figure 3.3	Electrically equivalent circuit model of a single cell.	29
Figure 3.4	Tensile strength graph.	30
Figure 3.5	The four-probe electrical bioimpedance measurement.	31
Figure 3.6	Paraffin embedding and tissue sectioning processes.	33
Figure 3.7	A picture from our study showing an Hematoxylin Eosin stained tissue sample.	33
Figure 4.1	Proliferation rate of control group samples. Increased relative absorption values have shown the proliferation of non-irradiated control cells.	36
Figure 4.2	MTT assay cell viability results of 635nm laser irradiated L929 cells 24, 48 and 72 hours after the irradiations.	37
Figure 4.3	MTT assay cell viability results of 809nm laser irradiated L929 cells 24, 48 and 72 hours after the irradiations.	37
Figure 4.4	1 J/cm^2 irradiated tissues compared to the control group samples.	38
Figure 4.5	3 J/cm^2 irradiated tissues compared to the control group samples.	38
Figure 4.6	Tensile strength measurement results of 635 nm irradiated samples after the 3, 5 and 7 days following irradiations.	40
Figure 4.7	Tensile strength measurement results of 809 nm irradiated samples after the 3, 5 and 7 days following irradiations.	41
Figure 4.8	Electrical resistance values of control group, laser irradiation groups and intact skin samples from the lowest to the highest frequencies of measurement (10kHz - 1MHz) on the 3^{rd} day of healing.	42
Figure 4.9	Electrical reactance values of control group, laser irradiation groups and intact skin samples from the lowest to the highest frequencies of measurement (10kHz - 1MHz) on the 3^{rd} day of healing.	42
Figure 4.10	Electrical resistance values of control group, laser irradiation groups and intact skin samples from the lowest to the highest frequencies of measurement (10kHz - 1MHz) on the 7^{th} day of healing.	43

Figure 4.11 Electrical reactance values of control group, laser irradiation groups and intact skin samples from the lowest to the highest frequencies of measurement (10kHz - 1MHz) on the 7^{th} day of healing. 43

Figure 4.12 Electrical resistance values of control group, laser irradiation groups and intact skin samples from the lowest to the highest frequencies of measurement (10kHz - 1MHz) on the 10^{th} day of healing. 44

Figure 4.13 Electrical reactance values of control group, laser irradiation groups and intact skin samples from the lowest to the highest frequencies of measurement (10kHz - 1MHz) on the 10^{th} day of healing. 44

Figure 4.14 Electrical resistance values of control group, laser irradiation groups and intact skin samples from the lowest to the highest frequencies of measurement (10kHz - 1MHz) on the 14^{th} day of healing. 45

Figure 4.15 Electrical reactance values of control group, laser irradiation groups and intact skin samples from the lowest to the highest frequencies of measurement (10kHz - 1MHz) on the 14^{th} day of healing. 45

Figure 4.16 Average values of electrical resistance of each tissue sample at relatively low and high frequencies. Control group samples had higher resistance compared to laser treatment groups and intact skin for the 3^{rd} and 7^{th} days of healing. Following the 7^{th} day of healing resistance of both control group and laser group samples came close to that of healthy intact skin. On the 10^{th} and 14^{th} days, there was no remarkable difference between any of the groups and intact skin. Statistical evaluations were done using Kruskal-Wallis non-parametric test with a significance level of $p < 0.05$ (* indicates significance between groups). 46

Figure 4.17 Cole-Cole diagrams of intact skin samples on the 3^{rd}, 7^{th}, 10^{th} and 14^{th} days of healing. 46

Figure 4.18 Hematoxylin and eosin stained incisional wound samples. 48

Figure 4.19 Hematoxylin and eosin stained tissue samples on 3^{rd} day and 14^{th} days of healing. A Day 3 - Control (a Early granulation tissue, b Healthy peripheral tissue, c Dense collagenous fascia tissue, d Scab formation). B Day 3 - L1 group (a Early granulation tissue, e Incomplete reepithelialization, d Scab formation). C Day 3 - L2 group (a Granulation tissue, b Healthy peripheral tissue, c Dense collagenous fascia and striated muscle, d Scab formation). D Day 14 - Control (g Early scar tissue with higher amount of collagen, h Reepithelialization, c Dense collagenous fascia tissue). E Day 14 - L1 (g Early scar tissue, h Reepithelialization). F Day 14 - L2 (g Early scar tissue, b Healthy peripheral tissue, h Reepithelialization). Scale bars represent 500 μm. 51

Figure 4.20 Semi-quantitative evaluation of histological examinations on the 3^{rd} day of healing. Statistical evaluations were done Analysis of Variance (ANOVA) with a significance level of $p < 0.05$ (* indicates significance between groups). 52

Figure 4.21 Semi-quantitative evaluation of histological examinations on the 7^{th} day of healing. Statistical evaluations were done Analysis of Variance (ANOVA) with a significance level of $p < 0.05$ (* indicates significance between groups). 52

Figure 4.22 Semi-quantitative evaluation of histological examinations on the 10^{th} day of healing. Statistical evaluations were done Analysis of Variance (ANOVA) with a significance level of $p < 0.05$ (* indicates significance between groups). 53

Figure 4.23 Semi-quantitative evaluation of histological examinations on the 14^{th} day of healing. Statistical evaluations were done Analysis of Variance (ANOVA) with a significance level of $p < 0.05$ (* indicates significance between groups). 53

LIST OF TABLES

Table 3.1	Irradiation parameters of 635nm and 809nm laser sources for laser groups.	28
Table 3.2	Tissue dehydration procedure.	32
Table 3.3	Scale for the semi-quantitative evaluation of histological examinations (GT-Granulation tissue ST-Surrounding tissue).	34
Table 4.1	Tensile strength measurement results at 3^{rd}, 5^{th} and 7^{th} days of healing.	39
Table 4.2	Percentage increase of resistance values of wound tissues at 100kHz compared to intact skin.	42
Table 4.3	Cole-Cole plot fit percentage of wound samples on each experiment day.	45
Table 4.4	Average wound areas (a,b indicating significant difference compared to the control group).	49

LIST OF SYMBOLS

A	Area
C_m	Cell Membrane Capacitance
f_c	Characteristic Frequency
L	Length
R	Electrical Resistance
R_e	Extracellular Fluid Resistance
R_i	Intracellular Fluid Resistance
X_c	Capacitive Reactance
V	Volume
Z	Electrical Impedance
α	Alpha
ω	Angular Frequency
ρ	Specific Resistiviy
σ	Conductivity
θ	Phase Angle

LIST OF ABBREVIATIONS

ANOVA	Analysis of Variance
ATP	Adenozin Trifosfat
CCO	Cytochrome C Oxidase
CTFG	Connective Tissue Growth Factor
DMEM	Dulbecco's Modified Eagle's Medium
ECM	Extracellular Matrix
EGF	Epidermal Growth Factor
FBS	Fetal Bovine Serum
FGF-2	Fibroblast Growth Factor-2
GaAlAs	Gallium Aluminum Arsenide
GaAs	Gallium Arsenide
GAG	Glycosaminoglycan
GRO	Growth Related Oncogene
GT	Granulation Tissue
H&E	Hematoxylin and Eosin
IL	Interleukin
LLLT	Low-level Laser Therapy
MIP	Macrophage Inflammatory Protein
MTT	3-(4,5-Dimethylthiazol-2-yl)-2,5 diphenyltetrazolium bromide
NGF	Nerve Growth Factor
PDGF	Platelet-Derived Growth Factor
PBM	Photobiomodulation
PBS	Phosphate Buffered Formalin
PMNL	Secreted Protein Acidic Rich in Cysteine
SC	Stratum Corneum
SPARC	Polymorphonuclear Leukocytes
ST	Surroinding Tissue
TGF-a	Transforming Growth Factors a

TGF-b	Transforming Growth Factors b
UV	Ultra Violet
VEGF	Vascular Endothelial Growth Factor

1. INTRODUCTION

1.1 Motivation

Wounding is the condition of a biological tissue, where its normal anatomical structure and function is defected completely or partially. Accordingly, wound healing can be defined as a complex process that the tissue endeavors to repair the defected area which will result in the restoration of anatomical structure and functional continuity by means of specific physical and chemical changes that begin immediately after wounding and last through the complex process [1, 2].

Photobiomodulation is a term used for defining the usage of low power laser irradiation on biological tissues aiming therapeutic effects while keeping the thermal effects as low as possible. It is critically important to choose the appropriate laser wavelength with power and energy levels to obtain the desired therapeutic consequences. The biostimulation effect of light is usually achieved by using light in the range of visible red to near infrared part of the electromagnetic spectrum, at a power density less than few hundreds of miliwatts [3–6]. On the other, hand energy density has been shown to be less than 50 J/cm^2 for obtaining stimulating effects of light irradiation. Biostimulation occurs by absorption of light energy by mitochondrial chromophores and photoreceptors in the cell membrane, causing the ground state electrons get excited and produce internal conversion energy. The absorption of light energy may result with enhanced enzyme activity and mitochondrial respiration, with increased ATP production [7–10]. In addition, it is stated that laser biostimulation with low energy density triggers the activation of intracellular signaling pathways and changes the similarity of transcription factors related to the proliferation of cells during tissue regeneration [11–14].

Wound monitorization is an important aspect in terms of quality of life especially for patients suffering from chronic non-healing wounds. It is crucial to follow the healing process in order to manage the treatment procedure properly. Recently, many research

studies have been investigating the wound treatment methods and materials, together with finding out modalities for monitorization of the complicated healing process in terms of cellular, molecular and biochemical changes. However, most of these methods are not only limited with accuracy, reliability and cost but they also lack of researcher objectiveness [15].

Complex bioimpedance measurement of biological tissues over a broad frequency range has been gaining wide popularity and considerable importance, not only for clinical diagnosis, but also fundamental research in determining pathological and physiological status and characterization of biological tissues in-vivo, in-vitro and ex-vivo [16–18]. Valuable information may be obtained with bioimpedance analysis in research applications about the status of tissues such as; skin hydration, ischemia, lung edema, skin cancer, dental decay, body fat content, tissue ischemia, blood viability [15, 19–25].

1.2 Objectives

1. To investigate the photobiomodulation of laser irradiation using visible red and near infrared laser sources at different energy densities on mouse fibroblasts in vitro and wound models in vivo.

2. To examine the changes in electrical impedance properties of tissues during the phases of wound healing in order to monitor the complicated process of healing by means of non-invasive multi-frequency bioelectrical impedance measurements.

3. To investigate the feasibility of bioelectrical impedance measurement as a tool for monitoring the biostimulation effect of laser application on skin wounds in vivo.

1.3 Outline

The first chapter gives the background information about laser biostimulation on wound healing and electrical bioimpedance measurements for wound healing monitorization.

In chapter 2, information about wound types and phases of wound healing are given in detail. This chapter continues with the principles of Photobiomodulation and Laser Biostimulation. Then, Electrical Bioimpedance Measurements for wound monitorization is introduced.

In chapter 3, experimental design of the whole study is given. Following the block diagram, laser biostimulation parameters on in-vitro cell viability and in-vivo cutaneous skin wounds were explained. The chapter continues with monitorization of the healing process by means of mechanical tensile strength tests, histological evaluations and electrical bioimpedance measurements.

In chapter 4, results of the experiments are given.

In chapter 5, the overall study is evaluated and discussions and conclusions of the results are given.

2. BACKGROUND

2.1 WOUND HEALING

Wounding and wound healing occur in all tissues of the body. Although general processes of healing are common to all tissues types, specialized tissues may have unique healing processes. For example, healing of liver tissue specifically is based on regeneration, rather than repair [26]. The chemical and physical changes occurring during a normal healing process of acute wounds can be examined under four distinct, but overlapping stages: hemostasis, inflammation, proliferation and remodeling. Normal healing starts at the beginning of the injury with the rush of the blood components into the damaged area.

2.1.1 PHASES OF WOUND HEALING

2.1.1.1 Hemostasis. During the hemostasis phase, it is important for the body to stop bleeding without inhibiting the normal blood flow. Macroscopically, tissue blanching and blood clot formation are the two important signs of hemostasis. In terms of cellular response, fibrin, platelets and blood vessel formation are microscopically observed [27]. The first macroscopically visible inflammatory response is blanching, which is the manifestation of vasoconstriction (narrowing of blood vessels). Vasoconstriction is initiated by the release of vasoactive amines, such as prostaglandins and thromboxanes, resulting with the contraction of muscular walls of the vessels [27–29]. This is a critically important response of the body for controlling bleeding and regulating the arterial blood pressure. On the other hand, it is known that epinephrine and norepinephrine secretion through the sympathetic nervous system also contributes the vasoconstriction [27–29]. The second inflammatory response is the platelet (thrombocytes) aggregation at the wound site, which is the part of the thrombus formation resulting with the blood clot formation at the target area. Platelets as being responsible for releasing the clotting factors are crucial not only for controlling bleeding but they also trigger the process of healing by providing

cytokines and growth factors [30, 31]. The aggregation of platelets leads to the release of alpha granules containing a variety of immunomodulation factors. These factors include albumin, fibrinogen, fibronectin and coagulation factors V and VIII, as well as platelet-derived growth factor (PDGF), transforming growth factors a and b (TGF-a and TGF-b), fibroblast growth factor-2 (FGF-2), and platelet-derived epidermal growth factors (EGFs), and endothelial cell growth factors [31–33].

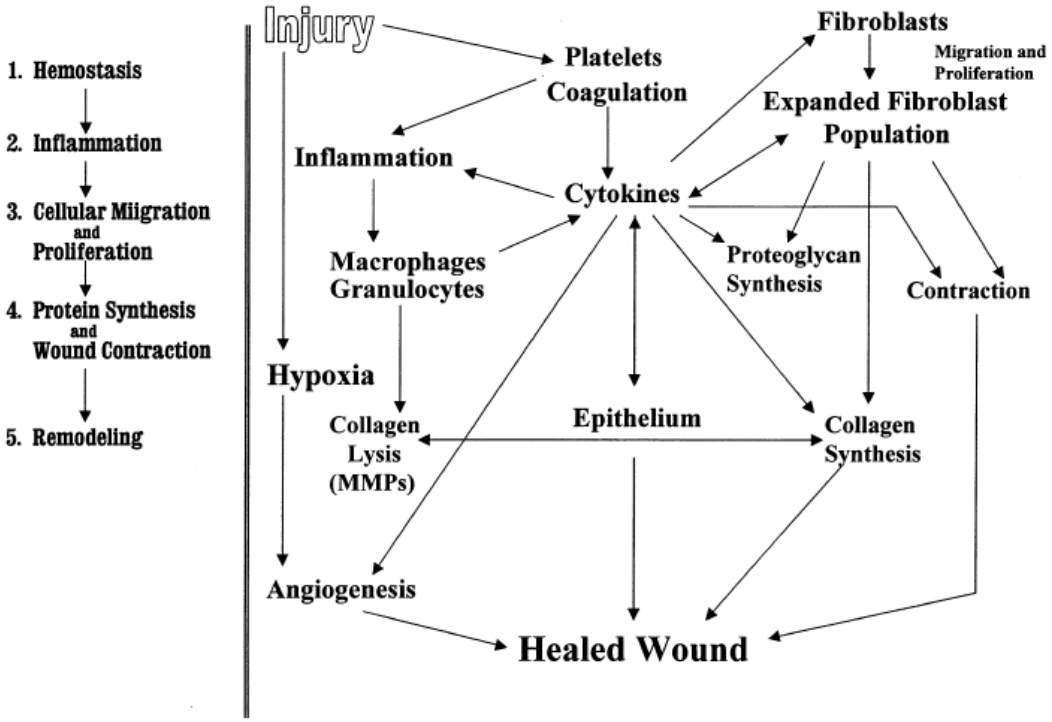

Figure 2.1 Events occurring during acute wound healing. The complex structure shows the interdependency of various events from the beginning to the final phases of healing. Cytokines play a central role in wound healing and serve as a central signal for various cell types and healing events [31].

The conversion of fibrinogen to fibrin due to the production of thrombin, which stimulates vascular permeability and extravascular migration of inflammatory cells, stabilizes the platelet plug by acting as a meshwork. Any inadequate fibrin formation or removal of fibrin from wound area delays wound healing process [34, 35]. Blot clot formation is the final product of this initial phase. It is primarily composed of platelet aggregation and fibrin mesh, which acts as a material that fibroblasts and other cells migrate during the healing process. Clot formation is critically important because it not only prevents further electrolyte and fluid loss along the wound area but also avoids contamination from the outside environment [31].

2.1.1.2 Inflammation. Inflammation (first introduced by Hunter in 1794) is characterized by the erythema, edema, heat and pain. Signs of inflammation start immediately after the wounding. The principal mechanisms of this early stage are the transfer of inflammatory cells through the wound area due to capillary vasodilation and migration of leukocytes into the extracellular matrix. Capillary vasodilation and increased permeability are both effected by antidromic stimulation of sensory nerves and permit the leakage of plasma to the extracellular area. This leakage is the main cause of signs of edema and pain [27, 36]. The first inflammatory cells that are attracted to the wound site by several growth factors and cytokines, such as plasma derived growth factor (PDGF), interleukin (IL)-8 and growth related oncogene (GRO)-alpha-CXCL1 chemokine ligand are the polymorphonuclear leukocytes (PMNL) [27, 37]. They are mainly responsible of destroying bacteria and eliminating debris remained from dead cells and foreign particles [38].

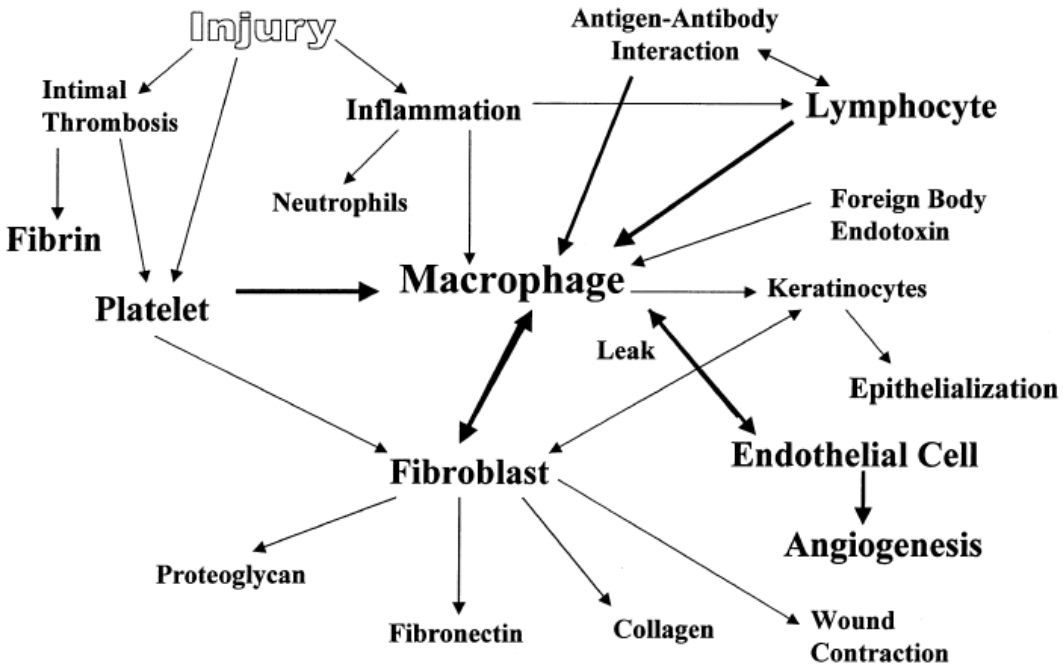

Figure 2.2 The complex relationship between various cell types and inflammatory markers during acute wound healing [31].

Following the invasion of PMNL cells at the wound site, monocytes rush into the target area and transform into macrophages. Similar to the leukocytes, macrophages also clean the wound area by removing cellular debris, bacteria and foreign particles. Compared to relatively shorter period of residency of the PMNL cells (24-48 hours), those macrophages stay at the wounded area for a longer period (days to weeks) [27]. However,

macrophages have much more responsibility. Macrophages are attracted to the wound site by release of growth factors, such as PDGF, TGF-α , nerve growth factor (NGF), TGF-α and macrophage inflammatory protein (MIP)-1α. Following their activation at the wound site, macrophages stimulate the secretion of again several growth factors (FGF-2, TGF-β and IGF), which stimulate the fibroblasts to produce collagen. Then, fibroblasts differentiate to myofibroblasts by TGF-β secretion from macrophages. In addition, angiogenesis and reepithelialization are also stimulated by macrophages through the release of TGF-α, FGF-2, TGF-β and IGF growth factors [27, 37]. Therefore, depletion of macrophages causes poor healing completion due to delayed fibroblast proliferation and angiogenesis resulting in insufficient fibrosis. At the late inflammation phase of healing, lymphocytes are the last cells arriving the wound area. They are attracted to the wound by the action of cytokines, i.e. interleukin-1 (IL-1), which play an important role in collagen remodeling and production of extracellular matrix components [39–42].

2.1.1.3 Proliferation. When the hemostasis and inflammation phases are successfully achieved, proliferative phase of healing, which is based on tissue repair takes place [39–42]. This phase usually starts on 3^{rd} day of healing and lasts for about 2 weeks. It is usually characterized by proliferation and migration of fibroblast, myofibroblasts production, deposition of newly formed extracellular matrix composed of fibrin and fibronectin, reepithelialization and angiogenesis. Macroscopically, this matrix is observed as the formation of granulation tissue [27, 39]. The permanent components of dermis following the start of proliferation are the fibroblasts, collagen (produced by fibroblasts), and blood vessels.

i. Fibroblast Migration and Production of Extracellular Matrix

Fibroblasts and myofibroblasts in the surrounding tissue are stimulated to migrate into the wound area. They are not only the factors TGF-β, CTGF, NGF and PDGF released by inflammatory cells and platelets and attract the fibroblasts into the wound area, but also fibronectin, which is another provisional matrix component, that stimulates the fibroblast migration into the wound area [27, 37, 43]. When fibroblasts appear in the

wound, they start to produce matrix proteins fibronectin, proteoglycans and type 1 and type 3 procollagen [39]. In unwounded healthy skin 80 to 90 percent of the dermal collagen is type 1, whereas remaining 10 to 20 percent is type 3. Collagen provides strength to the wounded tissue and facilitates the movement of endothelial cells and macrophages during the healing process [31].

Fibroblasts are the most important mesenchymal cells involved in wound healing due to their two basic roles of factory and machinery. They are the factories producing the collagen-based extracellular matrix (including collagen, glycosaminoglycan [GAG], and proteoglycans) that will replace the provisional fibrin-based matrix and growth factors, and are machineries as they contain thick actin bundles below the plasma membrane and approximate the wound edges through their contractile properties [27, 39]. Thus, it is critically important to mention that fibroblasts are involved in the complicated healing process by not only producing collagen but they also regulate the growth and function of other cells and are responsible for production of various cytokines and growth factors (IL-1 and TNF-α stimulation PDGF release, NGF stimulating nerve ingrowth and keratinocyte proliferation) [27, 37]. Proteoglycans are polypeptide chains attaching to varying structures of GAGs and serve together as information messengers that regulate cells, cytokines, growth factors and other soluble proteins within the extracellular matrix (ECM) [27, 44].

ii. Angiogenesis

Angiogenesis is the process by which damaged blood vessels are replaced by new ones in the wounded area. Although angiogenesis takes place concurrently during all phases of the healing, it becomes more active from day 2 following wounding [27, 31, 39]. Angiogenesis is usually stimulated by changes occurring in the tissue environment, such as decreased pH level, increased lactate and low oxygen tension and regulated by means of several growth factors (VEGF, FGF, angiopoietin, and TGF-β) and cytokines produced during the inflammatory phase of healing [27, 45]. Angiogenesis is significantly affected by proteoglycans and the arrangement of ECM. Initially, perfusion supply along the wound area is limited with the number of undamaged vessels. Than, due to the invasion of many newly formed capillaries surrounding wound edges, vascular supply and blood flow

at the wounded site improves [39]. Immature capillaries initially are quite porous, which is a structure stimulated by VEGF. Under normal conditions, angiopoiteins stimulate the capillaries become non-porous and non-leaky during their maturation process [27,46]. Thus, although many growth factors mostly promote angiogenesis, some may participate the process in a totally different way [27]. Concurrently, endothelial migration is one of the other important events occurring after day 2 of healing. Endothelial migration is also stimulated by VEGF, FGF, angiopoietin, and TGF-β.

iii. Reepithelialization

Reepithelialization, which starts from the wound edges within a few hours following wounding, is another important event of the proliferative phase of healing. It simply is based on the reestablishment of intact epidermis over the granulation tissue following sloughing of residual eschar [27]. Following the increased epithelial cell activity around the wound edges, cells are attached to the provisional matrix [39]. During the reepithelialization, migration of keratinocytes across the granulation tissue leaves a stratified layer that continues until the opposite sides of the wound reestablish the contact back. This is known as the contact guidance [27,47]. The keratinocytes involved in this process are usually derived from two main locations: one from the cells from close proximity to the wound and the other is from the nearby hair bulges. It has been shown I recent studies that hair bulges are the reservoirs for keratinocyte stem cells. Similar to the stimulation other cells involved in wound healing, keratinocytes are also stimulated to migrate, proliferate and differentiate by many alterations among the environment, and cytokines and growth factors. These may include decreased calcium and increased magnesium levels, pH changes and hypoxia [27,48–50]. On the other hand, some of the growth factors and cytokines that are known to be involved in reepithelialization are TGF-β, FGF-2, FGF-7 and FGF-10 [27,37].

iv. Protein synthesis and wound contraction

Protein synthesis and wound contraction are two significantly important factors that changes the strength of a wound during healing. They both usually start after 4-5

days following wounding and last until the wound closure (usually about 2 weeks). Approximately 25 percent of total body protein and more than 50 percent of the protein in scar tissue is in collagen and it is critical to produce enough amount of collagen for better wound healing. As mentioned earlier, collagen synthesis is done by fibroblasts, which is stimulated by release of TGF-β, PDGF and EGF [31,51–53]. As the proliferation continues, new synthesized collagen and other proteins such as proteoglycans, thrombospondin I and SPARC (secreted protein acidic rich in cysteine) replace fibrin and fibronectin, which are the initial provisional components of the matrix. The contraction rate of a wound varies depending on the anatomic location, shape and type of the wound. However, in many cases it is predictable due to the looseness of the skin, which is approximately 0.6 to 0.7 mm per day [31]. Wound contraction depends strongly on myofibroblasts content along the wound area. Myofibroblasts derive from fibroblasts and they include actin-rich microfilaments in their cytoplasm, their nuclei are multi-lobulated and include abundant rough endoplasmic reticulum [31,54]. Gabbiani, who first introduced that myofibroblasts are modified fibroblasts, suggested that myofibroblasts are the "motor" cells that contract a wound. However, recent studies have demonstrated that fibroblasts in the central part of a wound may be more critical for the contraction [31,55].

2.1.1.4 Maturation. The final phase of wound healing, remodeling phase is based on the development of new epithelium and scar tissue formation. The clinical signs of maturation phase are wound contraction, increased strength, decreased redness and decreased thickness. Although in many cases starting of maturation may take more than even several months depending on the type, size and location of the wound, the initial signs are usually observed to overlap with the production of granulation tissue during the proliferation phase [27]. The rate of collagen synthesis diminishes and reaches the rate of collagen breakdown comes into a steady state with the synthesis about 3 weeks after the wounding [31, 39, 42]. Besides, the connective tissue bring the margins of the wound site closer with the regulation of inhibitory factors, PDGF, TGF-β and FGF [39]. Finally, with the decreased metabolic activity, fibroblast and macrophage density at the wound area reduces, growth of the capillaries stops reducing the blood flow to the wound area [27, 39, 56, 57].

Wound contraction starts after 4 to 5 days following wounding and lasts for about two weeks. Contraction is a process directly related to cell division which makes myofibroblasts critically important for the contraction of wound tissue because of their contractile properties due to the increased levels of actin filaments [27, 29][27, 29, 58]. The morphogenesis of fibroblasts into myofibroblasts 4 to 5 days after injury overlaps the initiation of contraction of the wound. The two important growth factors PDGF, TGF- are known to have a role in conversion of fibroblasts into myofibroblasts [37].

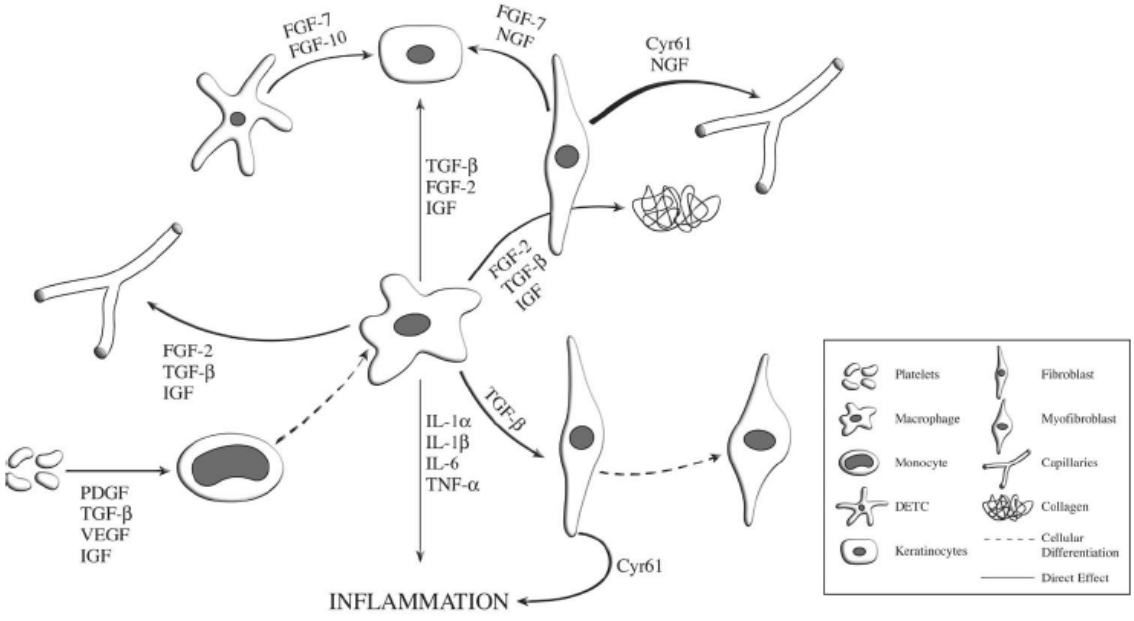

Figure 2.3 Schematic of the complex cellular and subcellular interactions of wound healing with the major participants, from inflammation to maturation [27].

2.1.2 WOUND TYPES

Wounds can be classified according to many parameters [26, 39]. Monaco et.al, states that, although there are variations in the healing process of different tissue types, the similarities between them are more than the differences [31]. According to the time of healing, wounds are clinically categorized as acute and chronic wounds [39]. Acute wounds repair themselves normally by following an ordered path of healing phases in terms of both functional and anatomical aspects. Therefore, healing of an acute wound follows a chain of predictable events. Basically, acute wound healing can be divided into five stages, which

are hemostasis, inflammation, cellular migration and proliferation, protein synthesis and wound contraction and remodelling [31]. They usually are the consequences of a traumatic loss of tissue or surgical procedure that usually lasts between 5 to 30 days depending on their size and location and patient criteria [26, 39]. Chronic wounds on the other hand are those, which do not succeed through the normal phases of healing process and are not repaired in a reasonable time interval. There are many factors that disturb the progress of healing and prolong one or sometimes more stages during the healing process. Some of them are infection, tissue hypoxia, necrosis, exudate and excess levels of inflammatory cytokines [39, 58].

The skin wounds, which has been especially under the focus of this study, are also classified as incisional wounds, excisional partial thickness and excisional full thickness wounds, which involve significant amount of tissue loss [31]. Wounds can heal by the application of sutures, tape or staples. This type of healing is called primary intention and has got minimum amount of scar formation. Secondary intention on the other hand is the healing of open wounds at which wound contraction, granulation tissue formation and reepithelialization leads the healing process. The seconder healing may end up with chronic wounds due to unsuccessful healing.

Researchers have been investigating therapeutic methods for managing the wound healing while trying to accelerate the healing process with various stimulation types, i.e., heat, light and electrical current. These modalities are thought to provide a potential treatment opportunity for chronic non-healing wounds and enhance the individuals' quality of life, which have been severely affected physically and emotionally. The conventional approach to wound management is based on applying medical agents to the wound such as antibiotics, medical plants, antiseptics and degerming products and wound dressings protecting the wound area from the external environment for preventing bacterial infections [59,60]. Nevertheless, with the findings of the recent studies on photobiomodulation, laser biostimulation on wound healing has gained great attention for the last couple of decades.

2.1.3 THE SKIN

The skin is a complex organ that covers the exterior of the body. It is the single largest organ both by sheer weight and surface area, accounting for approximately 15 percent of the total body weight. The functions of skin include protection of the inside of the body from the outside environment such that microorganisms, UV radiation, toxic agents and physical and chemical insults, regulation of the body temperature and prevention of excess amount of water loss from the body. The skin is a multi-layer structure consisting of epidermis, dermis and subcutaneous tissue [61].

2.1.3.1 The Epidermis. The epidermis is the outermost layer of the skin. It has a varying thickness from 0.05mm on the eyelids to 1.5-2mm on the soles of the feet and palm of the hand. It is a squamous stratified epithelium layer composed of mostly keratinocytes and also melanocytes, Langerhans cells and Merkel cells. Keratinocytes proliferate and divide in the epidermal basal layer and move up through the upper layers when they maturate. The epidermis is divided into four layers according to keratinocyte morphology and positions, which are the cornified or horny layer (stratum corneum-the outermost layer), the granular layer (stratum granulosum), the squamous layer (stratum spinosum) and the basal layer (stratum basale-the innermost layer) [62].

The stratum basale is the innermost layer of epidermis containing melanin-producing melanocytes and Merkel cells. Melanin pigment provides protection against UV radiation, which is attributed to the formation of many skin cancers. The melanin content of skin is directly proportional with exposure to light irradiation. Thus, the ratio of melanocyte to keratinocyte increases in facial skin compared to the other parts of the body. On the other hand, larger amounts of Merkel cells are found in the basal layer of skin parts with higher touch sensitivity as the fingertips and lips. As basal membrane cells reproduce and mature, they move towards the outer layers of the skin forming the stratum spinosum. The main content of this layer is the Langerhans cells. Theses immunologically active dendritic cells, which are derived from bone marrow act as antigen presenting cells and are large in number in the middle of the stratum spinosum. Following the maturation of

the cells, they continue to move towards the surface of the skin through stratum granulasum and stratum corneum. The outermost layer of epidermis, stratum corneum is made up of hexagonal-shaped layers of cornified cells. Varying thickness of stratum corneum is the main cause of varying thickness of the epidermal layer. It is approximately 10-20 um thick in general and can get as thick as 1.5-2mm. The structure of these cells provides the physical strength of the skin and a water-retaining barrier to the skin [62].

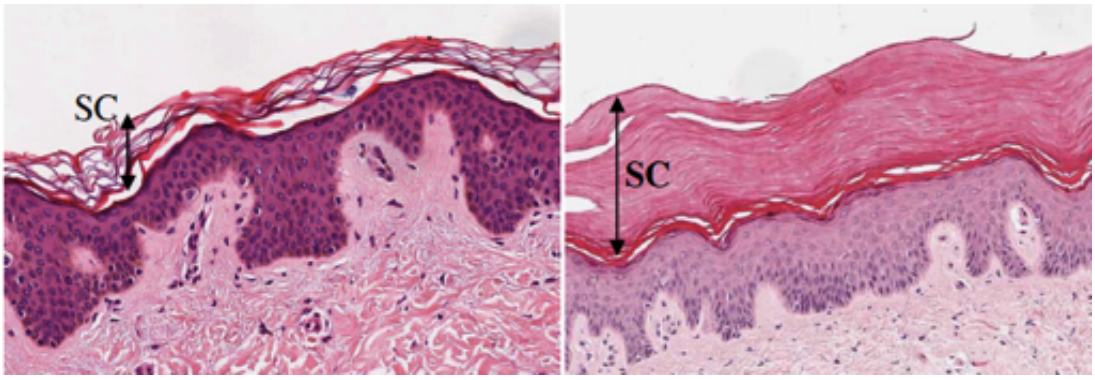

Figure 2.4 Varying thickness of Stratum Corneum [62].

2.1.3.2 The Dermis. Below the epidermis, there is the dermis with a thickness varying between 0.6mm on the eyelids and 3mm on the palms and soles of feet. The dermal layer has two main layers, a thin papillary layer and thicker reticular layer. Papillary dermis is the layer connecting the dermis with epidermis. It is mainly composed of loosely arranged collagen fibers. The reticular layer contains thicker collagen fibers running parallel to the skin surface and giving the strength and toughness of the dermis. The dermis is mainly made up of fibroblasts, which is responsible for collagen production, mast cells and macrophages with their roles in immune and inflammatory processes, sweat glands involved in temperature regulation, sensory receptors, sebaceous glands, blood vessels and hair follicles [62].

2.1.3.3 Subcutaneous Tissue. Underneath the dermis, the subcutaneous tissue (subcutis) consists of lipocytes, which are made up of fat storing cells and loose connective tissue. The high amount of fat content of this layer provides it function as a good insulator and physical barrier. Besides its fat content, there are also blood vessels and nerves inside subcutis.

2.1.4 Optical Properties of Skin

The optical properties of skin and the significance of skin pigmentation have been under the scope of research for more than a century [63]. The skin layers reflect and transmit light of different wavelengths in a different manner. Thus, optical properties of skin are determined by the varying optical properties of these layers separately. The main reason to the alterations of reflectance and transmission of light between those layers is the concentration of melanin, blood and keratin [63]. Light can be attenuated due absorption or scattering while passing through the matter.

The three primary absorbers of skin are blood, melanosomes and keratin [63–66]. Blood vessels are located below the epidermis, at which many of the optically triggered processes occur. However, due to the scattering properties of light, blood affects the amount of visible light and UV radiation reaching the epidermis. Therefore an increase in the absorption of radiation in the dermis due to increased blood concentration causes the back scattering of light through the epidermis. The decreased amount of radiation reaching the target molecules in the epidermal layers results causes a protection against incident radiation. The absorption of light at wavelengths longer than 600nm through blood is very low. This is the cause of red colour of blood.

The reflection and transmission of light between 300-700nm is strongly affected by also melanosome concentration and less affected at relatively shorter wavelengths around 280-300nm. Absorption is inversely proportional with wavelength for the UV part of the light spectrum. Below is the figure giving the relation between melanin concentration and reflectance and transmission of the stratum corneum and the entire epidermis at different wavelengths.

Keratin, which is the main component of nails and hair, is also one of the main components of the stratum corneum of epidermis. The production of keratin-rich cells causes the epidermis get thicker and provides protection against specifically UV radiation [63].

2.2 PHOTOBIOMODULATION

Photobiomodulation (previously phototherapy or low-level laser therapy-LLLT) refers to the use of low power laser irradiation on biological tissues for therapeutic purposes with minimal thermal effects. Laser therapy was first introduced by Endre Mester in 1967, due to unexpected results of hair growth of rats during the experiments, based on laser irradiation, and has been under the scope of scientific research for more than 30 years [3, 59]. Although there are more than a thousand studies on laser biostimulation published in the literature, there is still controversy on the stimulating effects of laser irradiation on biological tissues and the exact mechanism is not fully understood yet. Laser therapy is based on the mechanism of biostimulation, which is usually achieved by using visible red or near infrared wavelength light (390-1100nm) with an output power density of less than hundreds of miliwatts [3,6]. The energy density of the output beam is also relatively low, usually less than 50 J/cm^2 [67]. Research for the biostimulative effects of LLLT supports the idea that laser irradiation at appropriate doses may stimulate cell growth, proliferation and differentiation [67–70]. Because of the fact that energy transmitted via LLLT is very low, thermal effects due to the irradiation of those specific wavelengths may be considered negligible. It has been reported in literature that LLLT not only stimulates in vivo wound healing in terms of cellular response [1, 71, 72], but also appropriate wavelength of light irradiation can trigger cell activity in vitro [66, 73, 74].

The theoretical mechanism behind biostimulation is suggested to be through absorption of red and near infrared light in the tissue by mitochondrial chromophores, specifically cytochrome c oxidase (CCO) and photoreceptors in the plasma membrane of cells [11, 59]. This causes an electron of lower energy level to be excited and produce internal conversion energy. It is suggested that absorption of light energy may cause photo-dissociation of inhibitory nitric oxide from CCO leading to improved enzyme activity, electron transport, mitochondrial respiration and ATP synthesis [3, 10, 11, 75]. There are many studies published in literature supporting the biostimulation affects of laser irradiation. However, there are still uncertainties regarding the metabolic and cellular mechanisms between photon absorption and biological response of the organism against stimulation [11]. Because interaction of light with matter depends strongly on various

parameters such as, wavelength, power density, energy density, pulse mode and structure, coherency, time of irradiation, repetition and contact or non-contact irradiation and etc. [11]. It is not only the laser parameters that affect success of laser biostimulation, but proper target tissue preparation is also critically important. Any external agent specifically over the skin surface, or any physical condition of the patient that could inhibit healing procedure may be taken into account before the application. The range of wavelength usually preferred for treatment of superficial tissues is between 390nm and 600nm, whereas longer wavelengths have been used for their further penetration depths, however wavelengths in the range 700nm to 750nm are not often used due to their deficient chemical activity [11, 76, 77].

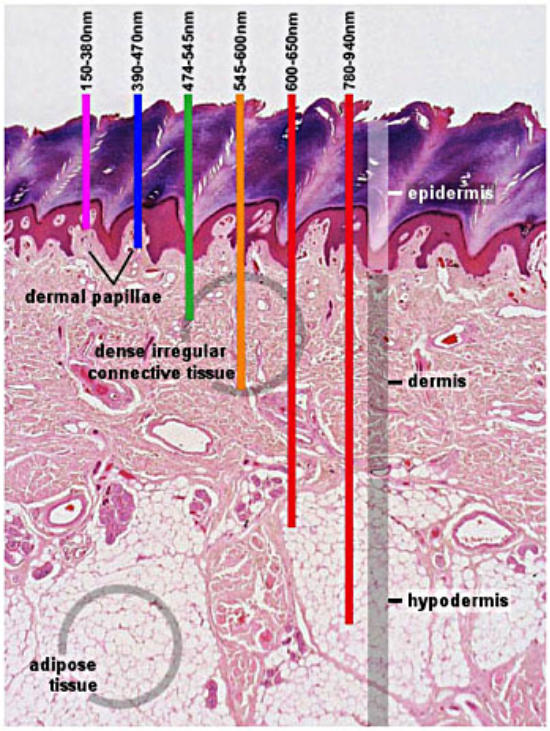

Wavelength (nm)	Color Range	Penetration (mm)
150-380	UV	< 0.1
390-470	Violet to Blue	0.3
475-545	Blue-Green	0.3-0.5
545-600	Yellow-Orange	0.5-1.0
600-650	Red	1.0-2.0
650-950	Red-NIR	2.0-3.0
950-1200	NIR	1

Figure 2.5 Penetration depth of light at various wavelengths through healthy skin [11].

Various light sources that have been used in laser biostimulation include inert gas lasers and semiconductor laser diodes such as helium neon (He-Ne; 633nm), ruby (694nm), Argon (488nm and 514nm), Krypton (521, 530, 568 and 647nm), Gallium Arsenide (GaAs; 904nm) and Gallium Aluminum Arsenide (GaAlAs; 612-879nm) [11,78]. Recently, reports indicate that 77 percent of laser wound healing studies have been performed on laboratory animals (87.5 percent of them were rats), 18 percent on cells and 4.8 percent of them used human subjects. Approximately 75 percent of those studies reported positive effect on

healing, whereas 25 percent had either no effect or negative results [59].

2.3 ELECTRICAL IMPEDANCE

Electrical impedance is a complex quantity that measures the opposition of a material against the flow of alternating electrical currents of various frequencies. It has real (Resistance, R) and imaginary parts (Reactance, X). It is can be expressed in the Cartesian form;

$$Z = R + jX \tag{2.1}$$

or the Polar form:

$$Z = Ze^{j\theta} \tag{2.2}$$

In polar form, Z is the amplitude of the complex impedance and phase angle θ is the time delay between the stimulating current and the voltage generated by that current. The mathematical relationship between Z, R and θ is shown in Figure 2.7.

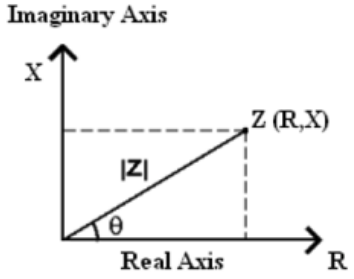

Figure 2.6 Graphical representation of the complex impedance.

$$R = |Z|\cos\theta \tag{2.3}$$

$$R = |Z|\sin\theta \tag{2.4}$$

2.3.1 BIOIMPEDANCE MEASUREMENTS

Biological tissues are generally modelled as simple uniform volume conductors. However, this is not the best way to represent any biological sample in terms of its electrical properties. There are various electrical equivalents that have been proposed so far, in order to describe the behaviour of biological tissues. Among those, three component models arranged in series and parallel combination are the mostly used ones. The series model has been used for describing the skin, whereas parallel combination has been used for more general purposes [79].

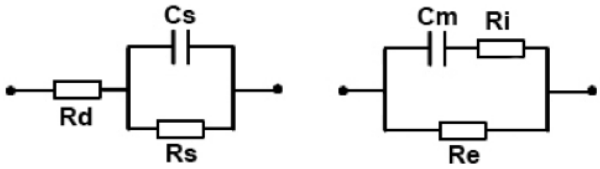

Figure 2.7 Three element equivalent models of a single cell in series and parallel combinations. In the first series combination model, Cs and Rs refer to the conductance created by the sweat ducts and resistance due to the outermost layer of the skin (stratum corneum). Rd in series represents the resistance of deeper layers. In the parallel combination model, Cm is the membrane capacitance, whereas Ri and Re are the resistances of intracellular and extracellular fluids respectively [79].

Tissues are composed of cells and extracellular fluid between cells. Those cells are enclosed by a cellular membrane, which controls the flow of ions in and out of the cell. Inside the cell membrane is the intracellular fluid. Both intracellular and extracellular fluids are highly conductive because of their high ion concentrations. Thus they represent the electrically resistive components of models. The lipid bilayer structure of the cell membrane is considered as a parallel plate capacitor with its trans-membrane protein channels acting like a dielectric interface between the bilayer.

The impedance measurements may reveal information about the cell population, cell membrane integrity and electrical conductivity characteristics of the intracellular and extracellular fluids of tissues [15,16,22]. Impedance measurements including the resistance (R) across the wound site and cell membrane capacitance (Xc) due to the lipid membranes, may be indicators of extracellular fluid (ECF) composition and cell membrane mass and function respectively [15], whereas cell membrane vitality may be indicated by the phase angle, which is calculated as the arc tangent of Xc/R ratio [15, 80, 81].

The conduction of electrical current through biological tissues is frequency dependent [16]. When an electrical current of low frequency is applied, cell membrane behaves highly resistant causing a low electrical current pass through the ECF resulting the impedance to be very high. When the current applied is increased to very high frequencies, the capacitive reactance of the membrane approaches zero. This causes the cell membrane act like a short circuit, and hence the current penetrates much more through the tissues, which decreases the impedance value to its minimum value [16].

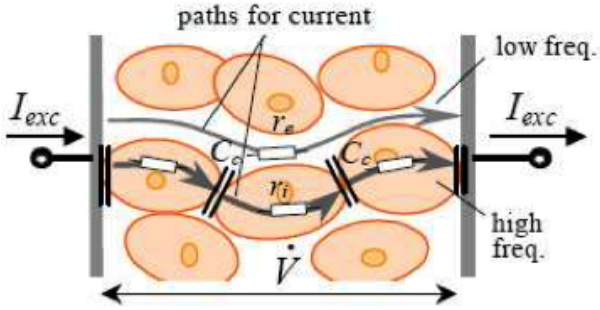

Figure 2.8 Frequency dependent response of biological tissues against an applied alternating current.

Therefore, bioimpedance measurements at a broad range of frequencies may be useful in detecting the clinical condition of tissues under investigation against the applied current during the phases of wound healing.

If we assume that the body is an electrical conductor in a cylindrical shape, the resistance of the body would be proportional to its length and inversely proportional to its cross-sectional area.

$$\mathrm{R} = \frac{\rho \mathrm{L}}{\mathrm{A}} = \frac{\mathrm{L}}{\sigma \mathrm{A}} = \frac{\sigma \mathrm{L}^2}{\mathrm{V}} \tag{2.5}$$

where ρ is the specific resistivity coefficient, σ is the conductivity, L is the length, A is the cross sectional area and V is the volume. However, since body is not a uniform cylinder, errors occur due to variations in the resistivity of the body parts and variations in the shape of the body and body segments. When a single cell is modelled as an electrical circuit, the characteristic behaviours of intracellular fluid, extracellular fluid and cell membrane can be given as below.

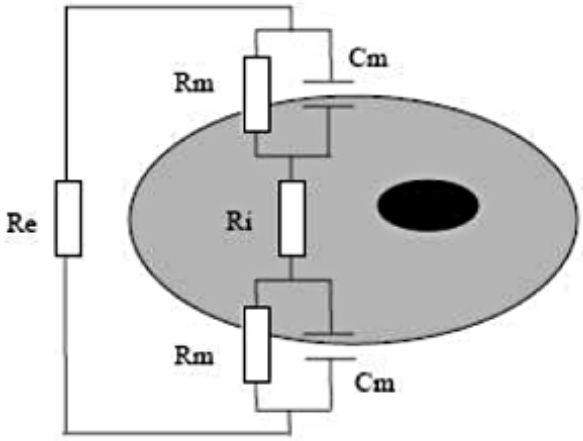

Figure 2.9 Electrically equivalent circuit model of a single cell.

where, *Re* represents the extracellular fluid resistance, *Ri* is the intracellular fluid resistance, *Rm* is the membrane resistance and *Cm* is the membrane capacitance.

Although there are many approaches regarding wound healing tracking, these methods are usually deprived without objectiveness and practicality [15]. The conventional methods with the limitations including cost and reliability may be supported by means of a new practical method for wound healing monitorization. Bioelectrical impedance analysis may be considered as a non-invasive and objective method that may provide safe and reliable information for the cellular and metabolic events during the healing process.

2.3.2 COLE-COLE PLOT REPRESENTATION

The complex series impedance of a single cell can be represented by the Cole-Cole plot, which is the depressed plot of the imaginary component against the real component of the impedance at different frequencies [16, 17, 82–85]. The Cole-Cole representation of the impedance provides the determination of the Cole parameters, namely R_0, R_∞, α and fc, where R_0 is the resistance at zero frequency, R_∞ is the resistance at infinite frequency and fc is the characteristic frequency [86]. The deviation from the pure capacitance is given by the experimental parameter α, which has a value between 0 and 1 ($\alpha = 1$; pure capacitance) [86]. The characteristic frequency of a RC element is the frequency at which the phase difference reaches its peak [87]. The frequency of measurements increases from right to left side of the plot. Thus, low-frequency data are at the right and high-frequency data are at the left part of the plot. The Cole-Cole parameters satisfy the equation;

$$\mathrm{Z} = \mathrm{R}_\infty + \frac{\mathrm{R}_0 - \mathrm{R}_\infty}{1 + (\mathrm{j}\omega\tau)^\alpha} \tag{2.6}$$

where $\omega = 2\pi f$and τ is the time constant. Once these parameters are obtained, then membrane capacitance C_m can be calculated from;

$$\mathrm{C_m} = \frac{1}{2(\pi)\mathrm{fC}(\mathrm{R}_0 + \mathrm{R}_\infty)^{\frac{1}{1-\alpha}}} \tag{2.7}$$

Measuring the impedance at zero frequency is important because at this frequency the cell membrane acts like an insulator and electrical current does not penetrate into the cells. Therefore, the value at zero frequency R_0 represents the impedance of the extracellular fluid alone. At very high frequencies on the other hand, reactance of cell membrane capacitance approaches zero and the overall impedance can be thought as the

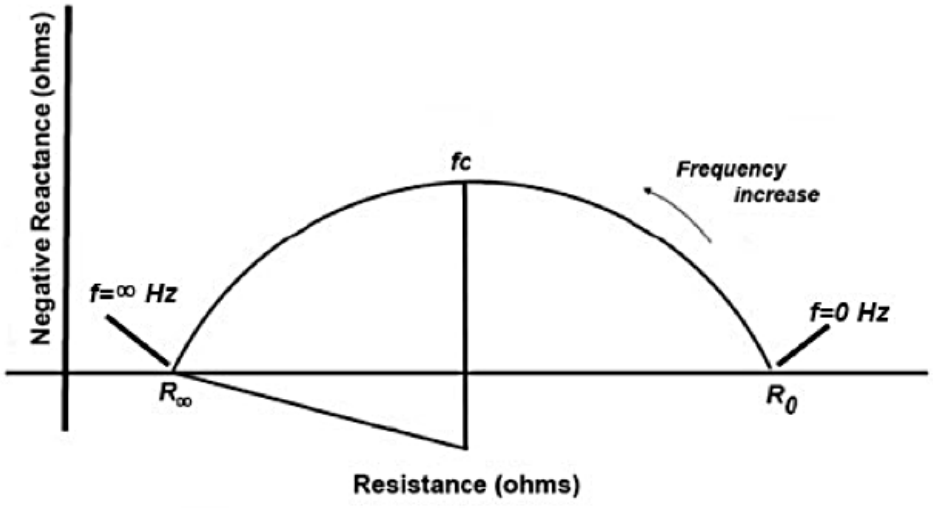

Figure 2.10 Cole-Cole plot diagram gives the frequency dependent relationship between the real (Resistance) and imaginary (Reactance) parts of the complex electrical impedance of biological tissues.

impedance of extracellular fluid connected in parallel with the intracellular fluid [87, 88].

3. MATERIALS AND METHODS

3.1 EXPERIMENTAL DESIGN OF THE STUDY

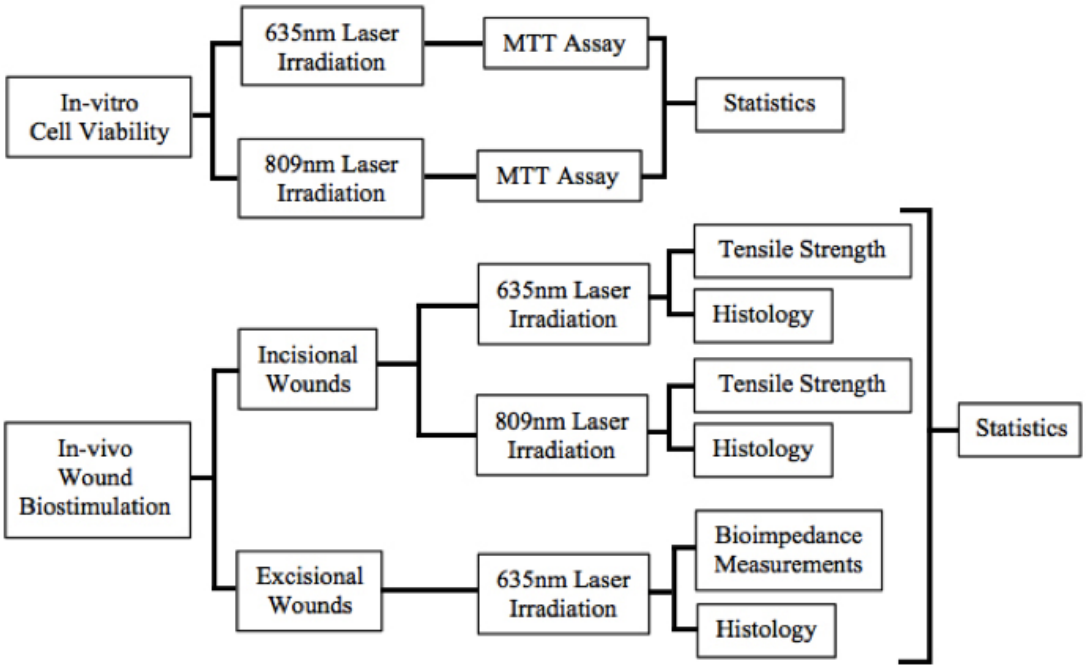

Figure 3.1 Experimental design of the study. In-vitro cell viability experiments were followed by in-vivo wound photobiomodulation experiments.

3.2 IN-VITRO CELL VIABILITY

3.2.1 CELL PREPERATION

L929 fibroblast cells obtained from the Molecular Biology and Genetics Department were grown in flasks containing Dulbecco's modified Eagles medium: Nutrient Mixture F-12 (Gibco) DMEM F-12 medium supplemented by 10% fetal bovine serum (FBS) and 1% antibiotic-antimycotic solution (Sigma). Incubations were in an environment of 5% CO2 and 95% air. The cells that reached 90% confluence were harvested after the treatment with 0.25% trypsin-EDTA solution (Sigma). The cells detached by this process were seeded in 96 well plates at a density of 105 cells per each well.

3.2.2 MTT ANALYSIS

Cell viability was examined with MTT (3-(4,5-Dimethylthiazol-2-yl)-2,5 diphenyl-tetrazolium bromide) assay protocol with a concentration of 5 mg MTT per 1 ml of PBS after 24, 48 and 72 hours following laser irradiation. DMEM (DMEM; Sigma-Aldrich, St. Louis, MO, USA) supplemented with 10% fetal bovine serum (FBS; Gibco, Grand Island, NY, USA), with 100 IU/ml penicillin, 100 μg/ml streptomycin and 2 mmol/l glutamine (Gibco) in an humidified incubator with 5% CO2 and 95% air at 37°C constant temperature. When an adequate number of cells were obtained, the cells were seeded on 96 well plates and kept in incubator for MTT analysis. Following the incubation, MTT solution was removed and replaced with 100 μl of DMSO. Well plates were mixed for 15 minutes. The absorbance values of the DMSO substrates were read by a commercial micro-plate reader (Bio-Rad iMark, USA). MTT assay was chosen for viability test, because MTT can only penetrate into the membranes of dead cells making it a simple method to distinguish between viable and dead cells.

3.3 IN-VIVO WOUND EXPERIMENTS

3.3.1 ANIMAL PREPERATION

The animal experiments were performed under a protocol approved by the Institutional Animal Research and Care Ethic Committee of Boğaziçi University (BUHADYEK, Date: 19.10.2012, No: 12XD4). Throughout the experiments, randomly selected male Wistar Albino rats, 3-4 months old and weighing 330 to 350 gr were used. The animal subjects were supplied by Vivarium, Center for Life Sciences and Technologies Research at Boğaziçi University. Rats were housed in plastic cages and maintained on a 12 hour light/12 hour dark cycle in a temperature controlled (22$\pm$2°C) room.

3.3.2 SURGERIES

i. Incisional Wounds

The rats (n=8) were subjected to general anesthesia (Ketamine 40 mg/kg, Xylazine 15 mg/kg). Three pairs of full thickness incisional wounds 1 cm long were made on the back of the animals, which were located symmetrically at both sides of the backbone parallel the spinal cord. The first pair was placed at the dorsal skin 5 cm posterior of the head and 1 cm at the lateral side of the spinal cord. The other pairs were placed 1 cm apart from each other. Three of the wounds were used for tensile strength measurements and three of them were used for histological examinations. Incisional samples were randomly selected for the histological examinations and mechanical tests at different locations on each rat in order to avoid any possible effect of motion artifacts caused by movements of animals during the healing process. In case of bleeding, wound site was compressed with sterile cloth and any blood remnant was removed to prevent possible light absorption by those blood remnants during the laser irradiations.

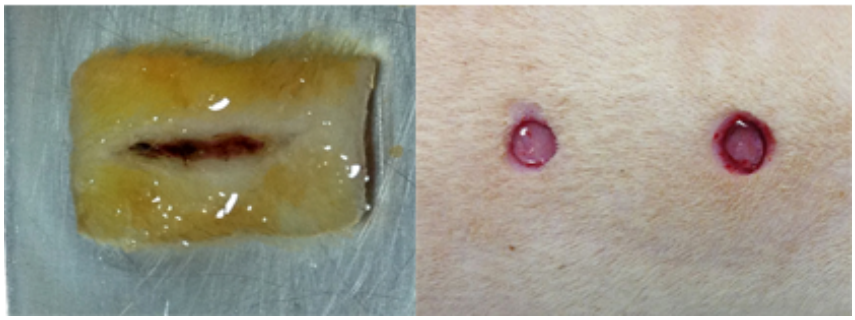

Figure 3.2 Incisional and excisional wound models.

ii. Excisional Wounds

The rats (n=32) were subjected to general anesthesia using same procedure of incisional wound surgeries (Ketamine 40 mg/kg, Xylazine 15 mg/kg). Following the anesthesia, three, round, full-thickness, skin wounds, 5 mm in diameter, were made on the back of each rat by means of punch biopsy. Hair at the wound site was shaved before wounding. One of the wounds was placed at the dorsal skin 5 cm posterior of the head and 1 cm at the lateral side of the spinal cord. The other two wounds were placed 1 cm apart

from each other. One of the three excisions of each animal was used as control wounds, which was not subjected to any laser irradiation. The other two wounds were classified as laser treatment wounds of two distinct energy densities. The wounds were chosen as control and laser treatment wounds randomly, similar to the procedure of incisional wound experiments, to avoid any possible effect of motion artifacts caused by movements of animals during the healing process.

3.3.3 POST SURGERY

Immediately after the wounding, laser irradiation was performed for once with the predetermined parameters and irradiation times. Both excisional and incisional wounds were left open for secondary healing, without the application of any external agent. The healing process was totally related to the natural response of the metabolism regarding granulation, reepithelialization and contraction. After the laser biostimulation experiments each animal was kept in separate cages during the secondary healing process until the days of histological examination or tensile strength test. The animals were sacrificed by cervical dislocation immediately after the removal of tissues for experimental studies.

3.4 PHOTOBIOMODULATION EXPERIMENTS

3.4.1 LASER IRRADIATION

The two laser sources used throughout the experiments were 635nm visible red laser light (VA-I-400-635, Optotronics-USA) and 809nm infrared diode laser (designed and developed at the Biophotonics Laboratory) [89]. These two laser sources were used separately for irradiating excisional and incisional wounds. Both lasers were used at two different energy densities of 1 J/cm^2 and 1 J/cm^2. Wounds were classified as Control (C), Laser 1 at 1 J/cm^2 (L1) and Laser 2 at 3 J/cm^2 (L2) groups. Laser beam of 1 cm in diameter was set to the output power of 50mW, where irradiation times for 1 and 3 J/cm^2 energy densities correspond to 20 and 60 seconds respectively. Laser output power was

checked with an optical power meter (Newport 1918-C, CA, USA) immediately before every experiment.

Table 3.1
Irradiation parameters of 635nm and 809nm laser sources for laser groups.

Group	Wavelength (nm)	Power Output	Treatment Time (s)	Energy Density (J/cm^2)
Incision-635-L1	635	50	20	1
Incision-635-L2	635	50	60	3
Incision-809-L1	809	50	20	1
Incision-809-L2	809	50	60	3
Excision-635-L1	635	50	20	1
Excision-635-L2	635	50	60	3

During the excisional wound stimulations with 635nm, laser output beam was adjusted for of 1 cm diameter in order to guarantee that all wounded area was exposed. The power output of the beam was set to 50 mW. Irradiation times for the two distinct energy densities (L1 and L2 groups) were 20 seconds and 60 seconds respectively (Table 3.1).

3.4.2 LASER SAFETY

Goggles filtering 809nm (LG1, Thorlabs, USA) were used for eye safety during the experiments.

3.5 TENSILE STRENGTH MEASUREMENTS

Tissue samples removed for tensile strength measurements were in rectangular shape covering the whole wound that had dimensions of 20mm x 25mm. Breaking

strengths of tissues were tested in less than ten minutes after the removal of tissues (Figure 3.4). During this time period, tissues were kept in 10% phosphate buffered formalin for avoiding the drying of the skin. The tissue samples were fixed between the jigs of a single column universal testing machine (LF Plus, Lloyd Instruments, UK) as close to each other as possible.

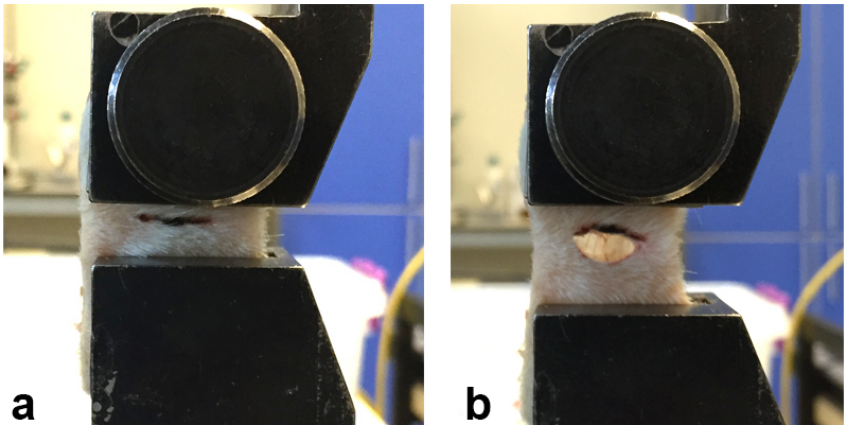

Figure 3.3 Electrically equivalent circuit model of a single cell.

The testing device was computer controlled using NexygenePlus software connected via RS232 connection. All specimens were preloaded at 5.5N and then were pulled vertically at a constant speed of 10mm/min, with a maximum load capacity of 250N, until the wound dehiscence was completed. Breaking strength values of tissues were recorded and tensile strength values were calculated from the breaking strength divided by the area of samples.

3.6 BIOELECTRICAL IMPEDANCE MEASUREMENTS

Multi-frequency bioimpedance measurements on each tissue sample were performed in-vivo on the 3^{rd}, $7^{t}h$, $10^{t}h$ and $14^{t}h$ days following the irradiations, by means of a conventional LCR meter, HP 4284A. In this study, tetra-polar (four electrode) measurement technique was preferred for eliminating the electrode-tissue interface [19, 20, 89, 90]. Two different stainless steel surface electrode pairs are used for current injection and voltage detection. Current electrodes 1cm apart from each other were placed on the peripheral healthy skin covering the wound site [Figure 3.5]. Current electrodes injected 1mA of

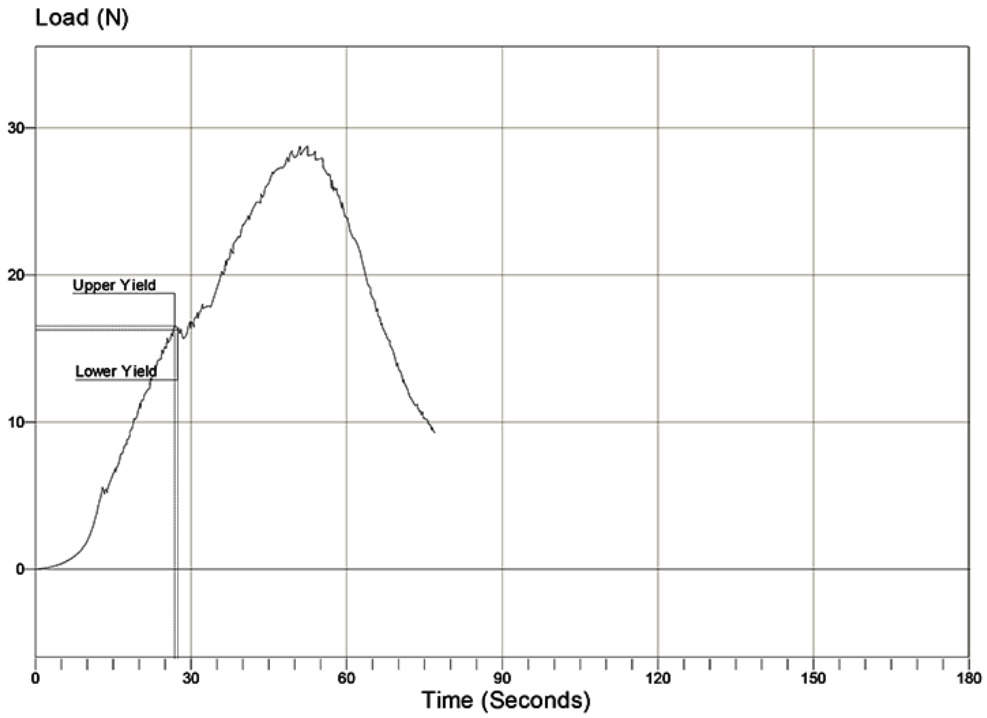

Figure 3.4 Tensile strength graph.

alternating current of varying frequency between 100 kHz to 1 MHz across the wound site. Voltage electrodes were placed at the margins of the wound area, 5 mm apart from each other.

With the electrical bioimpedance measurements, both electrical resistance and capacitive reactance values of target tissues at varying frequencies were obtained.

Electrical resistance and capacitive reactance values were determined for each measurement frequency were examined on Cole-Cole plots for investigating the response of tissue samples against electrical current of varying frequency. The measurements of each experimental group were repeated for eight times for statistical analysis.

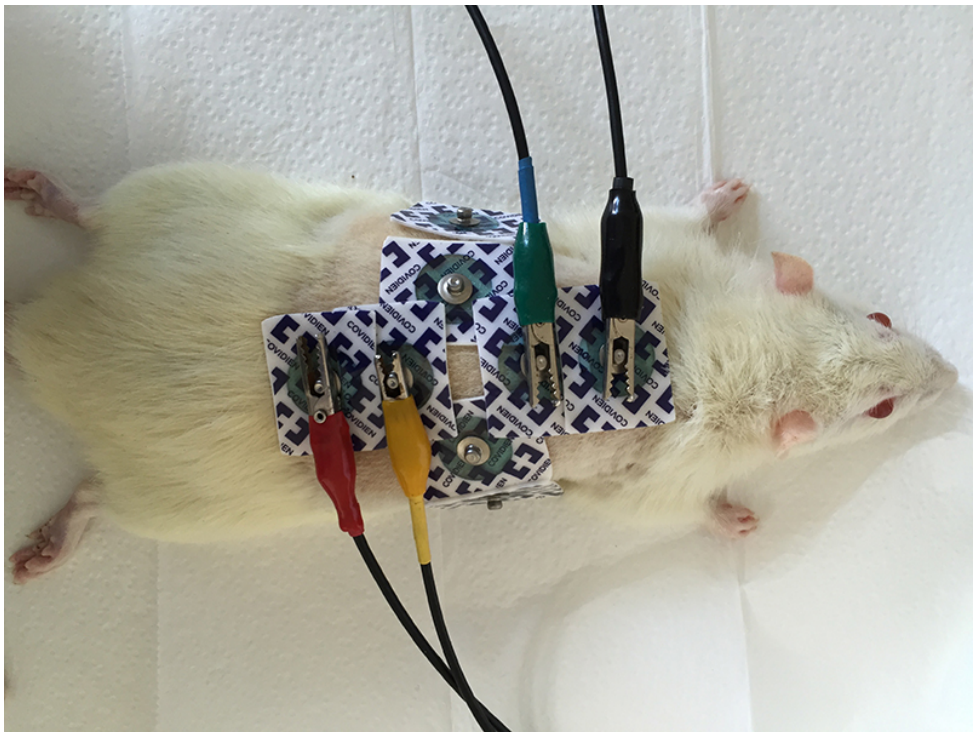

Figure 3.5 The four-probe electrical bioimpedance measurement.

3.7 HISTOLOGICAL EXAMINATIONS

3.7.1 TISSUE PROCESSING

Incision and excision tissue samples in rectangular shape (2 cm x 2 cm) covering the entire wound area were excised for morphological and histological examinations. Removed tissue samples were stored in 10% phosphate buffered formalin for 12 hours before tissue processing for fixation. The aim of tissue processing is dehydration of tissues and replacing the water content of samples with a medium that solidifies the samples in order to make them suitable for slicing in the order of micrometers. During the dehydration process, tissue samples are kept in predetermined baths for suitable intervals of time depending on the type of tissue. Basically, water content of tissues was removed by transferring the samples through baths of progressively increasing ethanol concentrations. This is followed by xylene, which is used for removing the alcohol and finally embedding in molten paraffin wax that replaces the xylene (Table 3.2). Tissue processing was done by means of a conventional processing machine (Leica TP-1020, Germany) at the Institute of Biomedical Engineering, Boğaziçi University.

3.7.2 PARAFFIN EMBEDDING

Tissues fixed in formalin and then embedded in paraffin may be stored at room temperature for a long time. After the tissue fixation procedure, tissues were embedded into heated liquid paraffin by means of an embedding device (Leica EG1150H, Germany). Cold plate at -5°C embedded to the hot plate was used for cooling the paraffin embedded blocks. The tissue samples were placed in cassettes oriented to enable sectioning cross sections of the samples.

Table 3.2
Tissue dehydration procedure.

Alcohol	70%	1 Hour
Alcohol	70%	1 Hour
Alcohol	80%	1 Hour
Alcohol	80%	1 Hour
Alcohol	90%	1 Hour
Alcohol	90%	1 Hour
Alcohol	100%	1 Hour
Alcohol	100%	1 Hour
Xylene		1 Hour
Xylene		1 Hour
Paraffin (60°C)		1.5 Hour
Paraffin (60°C)		1.5 Hour

3.7.3 TISSUE SECTIONING

Sectioning of tissue samples was done by means of a fully automated rotary microtome (Leica RM2255, Germany). Tissue samples were cut in a range of 6 to 16 micrometers thick. Then, sections and stretched in 40°C water bath, placed on glass slides and kept in incubator at 36 oC overnight for removing the excess paraffin remaining on the slides.

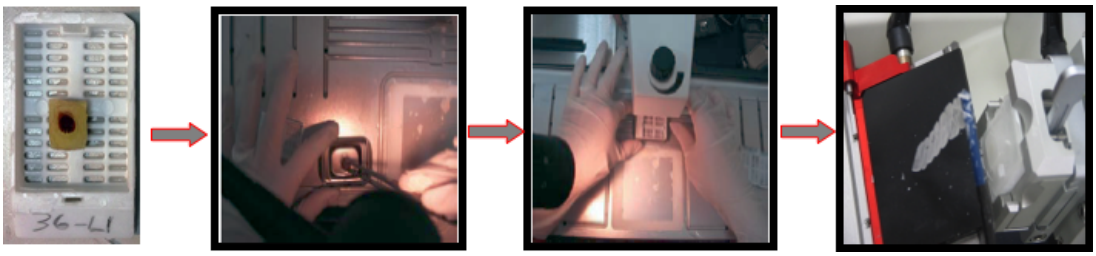

Figure 3.6 Paraffin embedding and tissue sectioning processes.

3.7.4 TISSUE STAINING

Hematoxylin and Eosin was used for staining the tissue samples. This is the most common used staining method in histology. Hematoxylin has a deep blue-purple color and stains nucleic acids, whereas eosin, which is an acidic dye, is pink and stains the cytoplasm and reticular and elastic fibers.

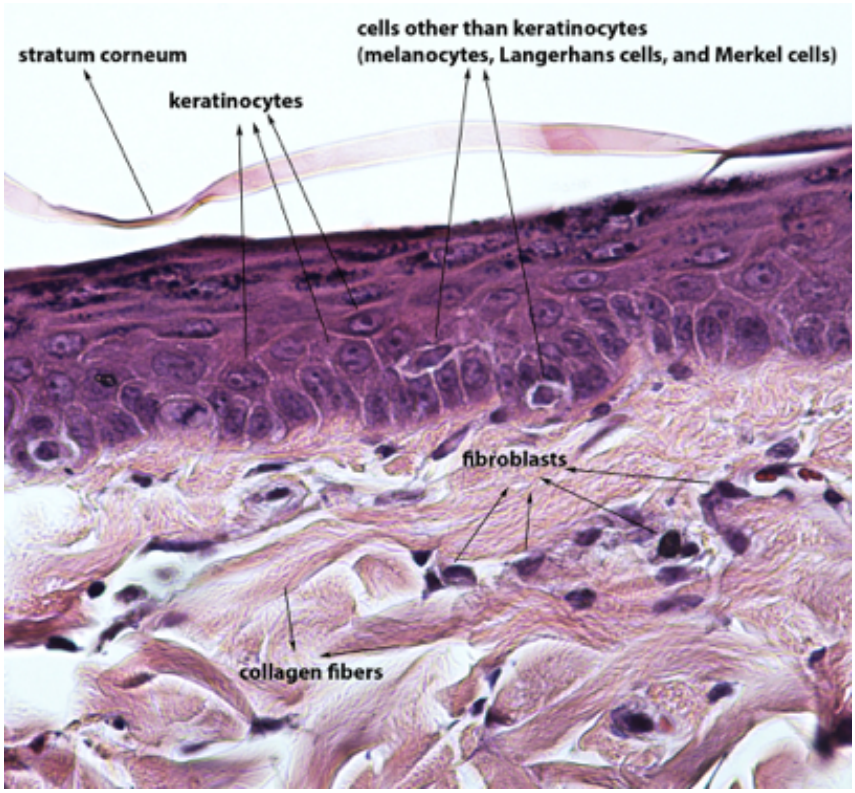

Figure 3.7 A picture from our study showing an Hematoxylin Eosin stained tissue sample.

3.7.5 HISTOLOGICAL EVALUATION

Semi-quantitative evaluations of the histological sections were done by a blind examiner by means of a conventional light microscope (Eclipse 80i, Nikon Co., Japan) according to the scale 0, 1, 2, 3 and 4 (Table 3.3).

Table 3.3
Scale for the semi-quantitative evaluation of histological examinations (GT-Granulation tissue ST-Surrounding tissue).

Scale	Epithelialization	Fibroblasts	Collagen	Angiogenesis
0	Absent	Absen	Absen-GT	Absent
1	Thickness of cut edges	Mild-ST	Minimal-GT	Mild-ST
2	Migration of cells	Mild-GT	Mild-GT	Mild-GT
3	Bridging of the excision	Moderate-GT	Moderate-GT	Moderate-GT
4	Keratinization	Marked-GT	Marked-GT	Marked-GT

3.8 STATISTICAL ANALYSIS

Semi-quantitative evaluation results of histological examinations were statistically checked using Analysis of Variance (ANOVA) method complemented with Tukey's test, with the significance level of $p < 0.05$. Statistical analysis of the bioimpedance measurement data were done by non-parametric Kruskal-Wallis test with the significance value of $p < 0.05$.

4. RESULTS AND DISCUSSION

4.1 IN-VITRO CELL VIABILITY

In order to understand the biostimulation effects of lasers on cell proliferation, cell cultures were irradiated with a diffuse light beam of power intensity of 50mW/cm2 at two distinct energy densities of 1 J/cm^2 and 3 J/cm^2 . Time of irradiations was 20 seconds and 60 seconds for 1 J/cm^2 and 3 J/cm^2 energy doses respectively.

Photobiomodulation transmits low-level energy, which principally causes negligible thermal effects. Hrnjak et al. supported the idea that temperature increase during LLLT experiments has been less than 1°C [50]. It has been confirmed by many studies that there was no remarkable change in temperature in fibroblast proliferation experiments [91, 92]. Schneede et al. also reported that laser irradiation at 40mW/cm2 power density caused an increase in temperature less than 0.065°C [93].

Before investigating the photobiomodulation of laser irradiations on cell cultures, proliferation of non-irradiated control cells was examined. L929 mouse fibroblast cells were cultured with approximately the same number of cells in each well. The cells were trypsinized and suspended in equal volumes of growth mediums. MTT assay analysis was performed at 24th, 48th and 72nd hours (Figure 4.1).

After observing the natural proliferation of non-irradiated control cells in their growth medium, second part of the experiments, namely laser biostimulation on L929 cell cultures was performed. Preparation of cells and laser irradiation setups were described in the materials and methods section. In order to determine the incident laser energy dependence of cell proliferation, power density was kept constant at 50mW/ cm2 during the experiments.

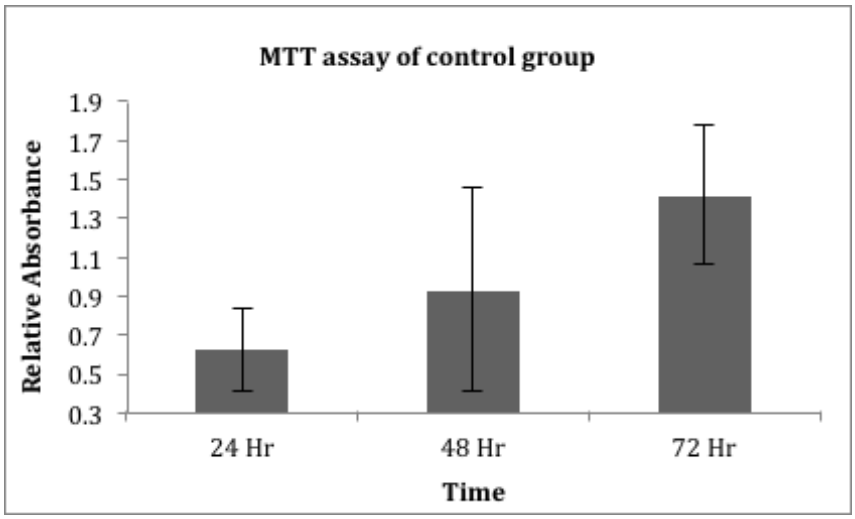

Figure 4.1 Proliferation rate of control group samples. Increased relative absorption values have shown the proliferation of non-irradiated control cells.

4.1.1 635 nm LASER IRRADIATION

MTT assay results obtained from 635nm laser irradiation groups 24 hours after the laser irradiations have shown the biostimulation effect of irradiation. The relative absorbance values of both L1 and L2 group cells (1 JJ/cm^2 and 3 J/cm^2 energy densities) were significantly higher than the non-irradiated control group cells ($p<0.05$) indicating that both energy densities had positive effect on viability of cells in-vitro during the first 24 hours. The effect for this early phase of proliferation was energy dose dependent. Proliferation due to higher energy dose (3 J/cm^2) was found to be greater than lower energy dose (1 J/cm^2). However, no significant difference was detected between these laser groups.

MTT assay results of 48th hour examinations did not show any difference between the groups. Both laser irradiation cells have shown same viability after 48 hours. We observed that 635nm laser irradiation at 1 J/cm^2 energy density significantly increased cell viability compared to non-irradiated control group samples after 72 hours following the irradiations.

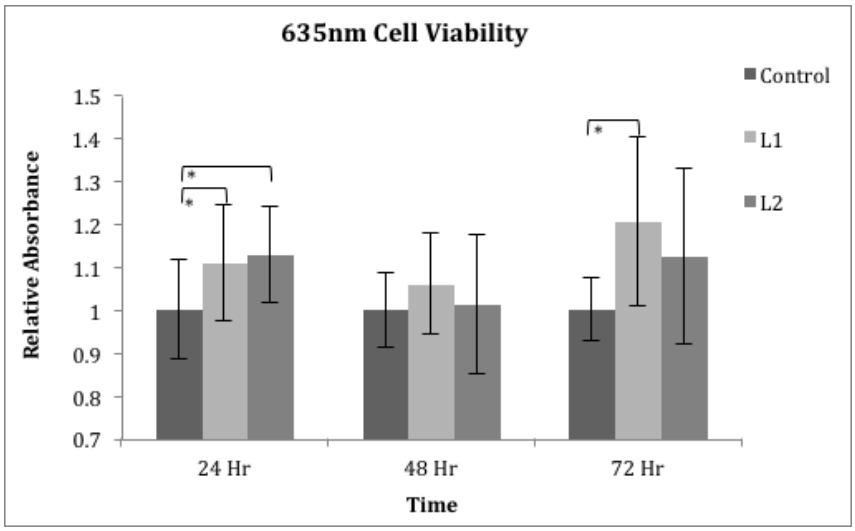

Figure 4.2 MTT assay cell viability results of 635nm laser irradiated L929 cells 24, 48 and 72 hours after the irradiations.

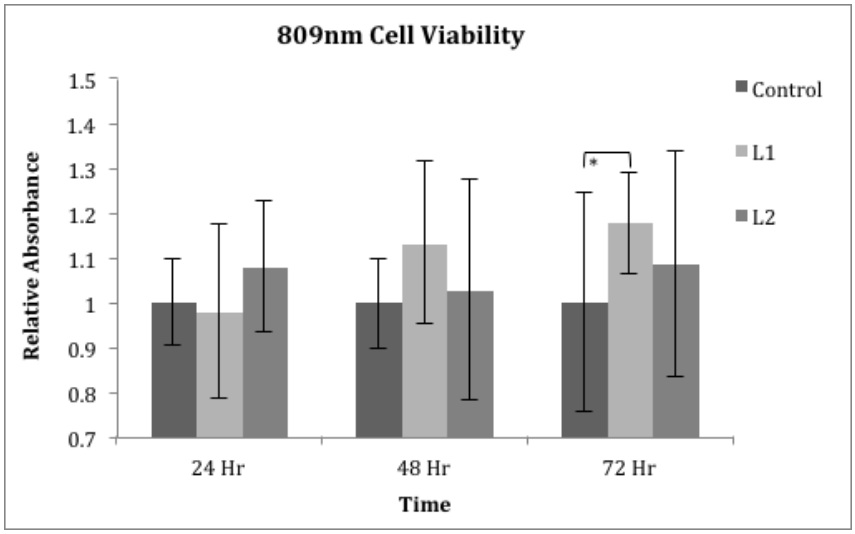

Figure 4.3 MTT assay cell viability results of 809nm laser irradiated L929 cells 24, 48 and 72 hours after the irradiations.

4.1.2 809 nm LASER IRRADIATION

809nm laser irradiation of both energy densities did not show any stimulation effect on cell viability at 24 and 48 hours after the irradiations. The only difference obtained was between 1 J/cm^2 laser irradiation group and control group samples at 72 hours analysis (Figure 4.2). Besides, both lasers had similar effects on cell viability in terms of proliferation rates at 48 and 72 hours, whereas 635nm irradiation of both energy densities was observed to be remarkably stimulative.

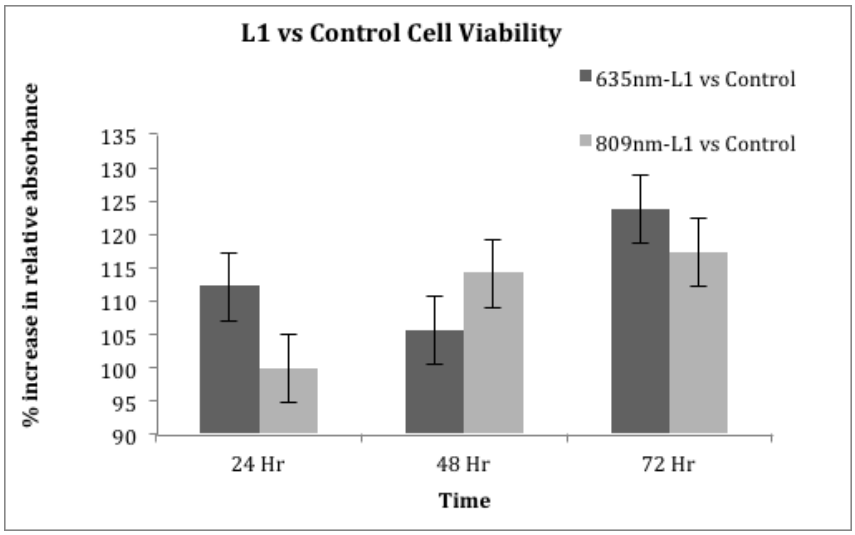

Figure 4.4 1 J/cm^2 irradiated tissues compared to the control group samples.

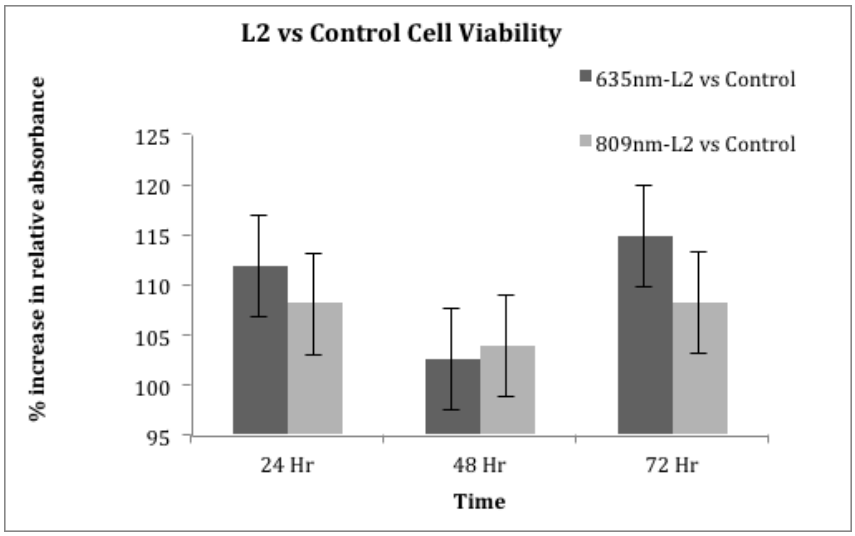

Figure 4.5 3 J/cm^2 irradiated tissues compared to the control group samples.

Comparison between the two wavelengths with the relative absorption values for each energy densities showed that 635nm laser stimulation was relatively more effective than 809nm wavelength, after 24 hours and 72 hours. But it was observed that cells exposed to 809nm laser irradiation had better viability values 48 hours after the applications.

4.2 TENSILE STRENGTH

4.2.1 635 nm LASER IRRADIATION

Tensile strength measurement results for all groups are shown in Table 4.2 below. On the 3^{rd} day of healing, neither 635nm nor 809nm laser irradiations of both 1 J/cm^2 and 3 J/cm^2 energy densities stimulated the healing process in terms of tensile strength. In terms of breaking strength, neither 1 nor 3 J/cm^2 laser irradiations of both wavelengths cause significant increase for the first 3 days of healing process. However, although the differences were not significant, 1 J/cm^2 laser irradiated samples were found to be slightly more effective than 3 J/cm^2 laser group samples (Table 4.1).

Table 4.1
Tensile strength measurement results at 3^{rd}, 5^{th} and 7^{th} days of healing.

Measurement Day	Group	635 nm	809 nm	Absolute Difference Between 635nm and 809nm
	Control	9.64 $\pm$1.78^a	9.91 $\pm$ 1.37^a	2.80
3^{rd} Day	1 J/cm^2	9.86 $\pm$ 3.02^a	11.96 $\pm$ 3.80^a	21.30
	3 J/cm^2	8.99 $\pm$ 2.1^a	10.32 $\pm$ 3.85^a	14.79
	Control	11.16 $\pm$ 3.06^a	11.65 $\pm$ 4.58^a	4.39
7^{th} Day	1 J/cm^2	16.93 $\pm$ 5.10^a	13.20 $\pm$ 5.13^a	22.03
	3 J/cm^2	12.45 $\pm$ 1.95^{a,b}	12.23 $\pm$ 3.11^a	1.77
	Control	12.65 $\pm$ 1.47^a	10.16 $\pm$ 1.90^a	19.68
10^{th} Day	1 J/cm^2	15.80 $\pm$ 2.35^a	12.28 $\pm$ 3.99^a	22.72
	3 J/cm^2	18.26 $\pm$ 1.56^a	12.31 $\pm$ 4.34^a	32.58

5^{th} day examination results of 635nm irradiated tissues showed that 1 J/cm^2 group incisions had significantly higher wound strength compared to non-irradiated control samples. However there was no remarkable increase of wound strength for 3 J/cm^2 group samples. Although 1 J/cm^2 laser group had more than 35 percent increased wound strength

compared to 3 J/cm^2, these two energy levels were not found to be statistically significantly from each other. On the 7^{th} day of healing, all of the incisions were closed and almost all of the strength values were quite close to each other. However, 3 J/cm^2 group samples showed increased wound strength compared to both control group and 1 J/cm^2 laser group samples.

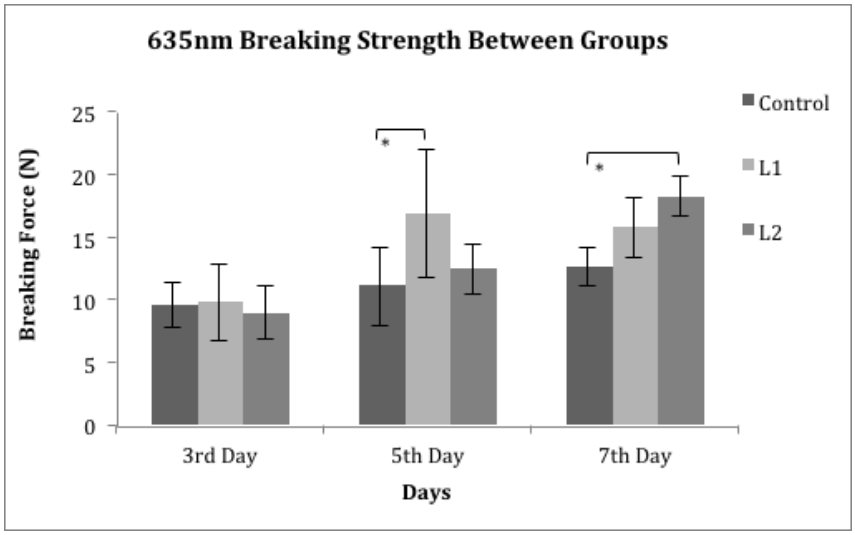

Figure 4.6 Tensile strength measurement results of 635 nm irradiated samples after the 3, 5 and 7 days following irradiations.

4.2.2 809 nm LASER IRRADIATION

809nm laser irradiation did not have any stimulation effect on any of the examination days. When these to wavelengths were compared, it is observed that 1 J/cm^2 energy density of 635nm laser irradiated tissues reached up to more than 30% higher wound strength than 809nm samples on the 5^{th} day of healing. But the difference was not high enough to cause a significant increase.

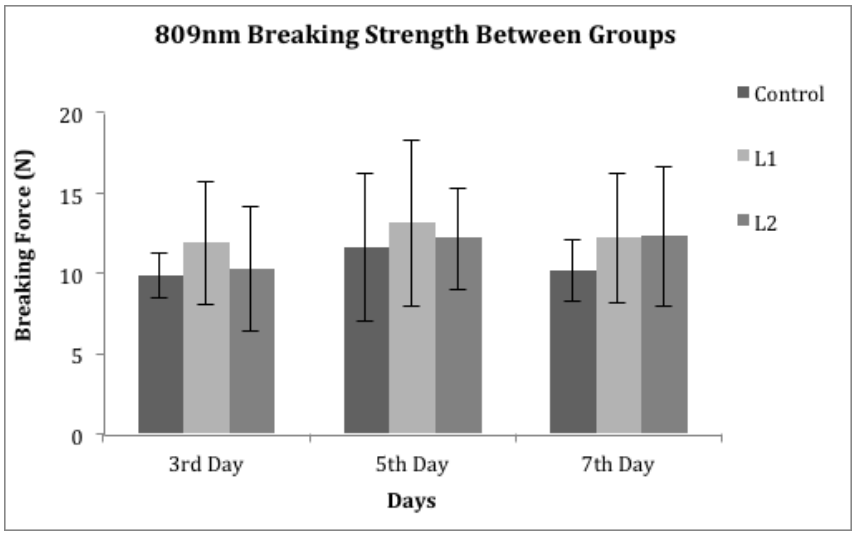

Figure 4.7 Tensile strength measurement results of 809 nm irradiated samples after the 3, 5 and 7 days following irradiations.

4.3 BIOELECTRICAL IMPEDANCE

4.3.1 BIOIMPEDANCE MEASUREMENTS

On the 3^{rd} day of healing, control group tissues have shown greater electrical resistance compared to both 1 J/cm^2 and 3 J/cm^2 laser irradiated samples and they were closer to the intact skin values. Below are the graphs showing the changes of electrical resistance and reactance values of non-irradiated control group, 1 J/cm^2 and 3 J/cm^2 laser irradiation group and intact skin samples from the lowest to the highest measurement frequencies (10kHz - 1MHz) on 3^{rd}, 5^{th}, 10^{th} and the 14^{th} days of healing.

The resistance values of all samples from both control and laser irradiation groups at lower frequencies increased until the 7^{th} day of healing and then decreases back until the 10^{th} day. Average resistance values of both control and laser irradiation group samples measured at 100 kHz are found to be remarkably higher than the intact skin resistance (Table 4.2).

The differences between those groups and intact skin values are found to decrease considerably after the 10^{th} day of healing with no remarkable differences between those groups showing that the electrical properties of excisions during the healing process are

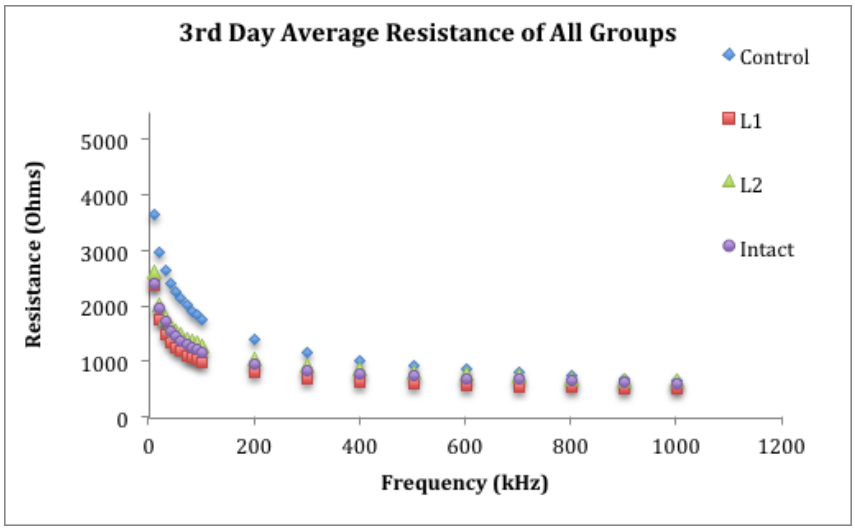

Figure 4.8 Electrical resistance values of control group, laser irradiation groups and intact skin samples from the lowest to the highest frequencies of measurement (10kHz - 1MHz) on the 3^{rd} day of healing.

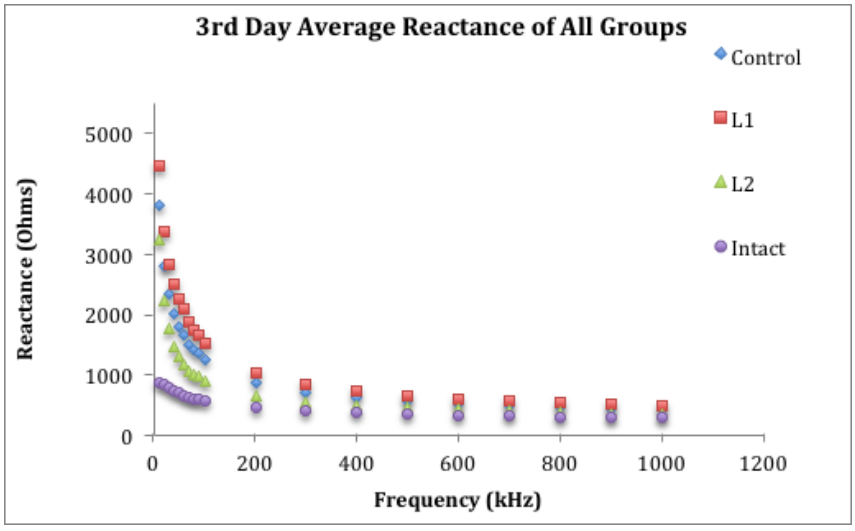

Figure 4.9 Electrical reactance values of control group, laser irradiation groups and intact skin samples from the lowest to the highest frequencies of measurement (10kHz - 1MHz) on the 3^{rd} day of healing.

Table 4.2
Percentage increase of resistance values of wound tissues at 100kHz compared to intact skin.

% Change of Resistance	3^{rd} Day	7^{th} Day	10^{th} Day	14^{th} Day
Control	49.9	99.2	31.2	11.6
1 J/cm^2	49.9	99.2	31.2	11.6
3 J/cm^2	32.8	69.7	36.1	7.3

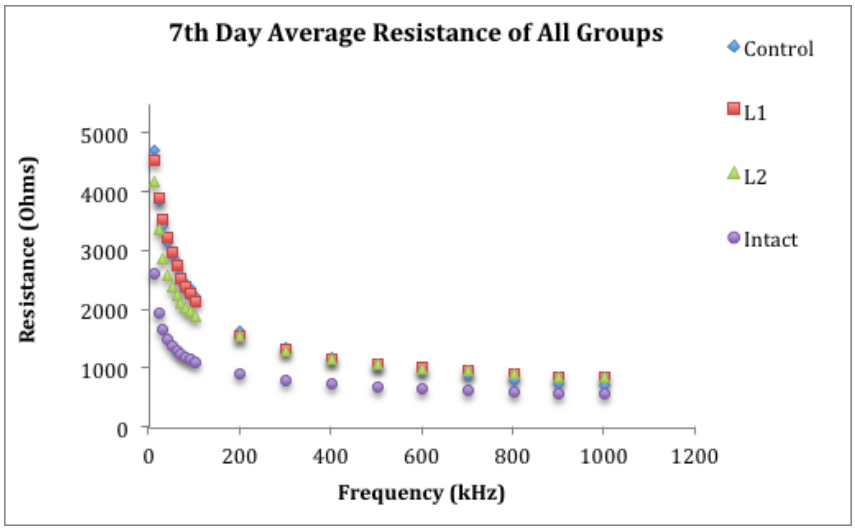

Figure 4.10 Electrical resistance values of control group, laser irradiation groups and intact skin samples from the lowest to the highest frequencies of measurement (10kHz - 1MHz) on the 7^{th} day of healing.

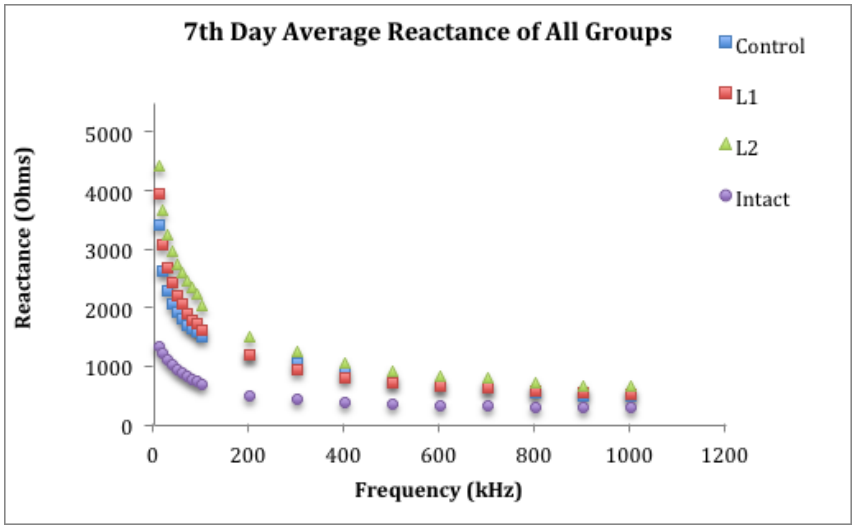

Figure 4.11 Electrical reactance values of control group, laser irradiation groups and intact skin samples from the lowest to the highest frequencies of measurement (10kHz - 1MHz) on the 7^{th} day of healing.

intercepting with the resistance of intact healthy skin. It has been observed that, reactance of wound samples for all groups increased until the 7^{th} day examinations similar to the changes of resistance values.

The completion of epidermal closure may have a great influence on those results after the 10^{th} day of healing. Because it has been shown already that continuity of the outermost layer of the skin, namely stratum corneum has a great influence on the resistance of skin [15]. The variation of resistance values of the experimental groups for

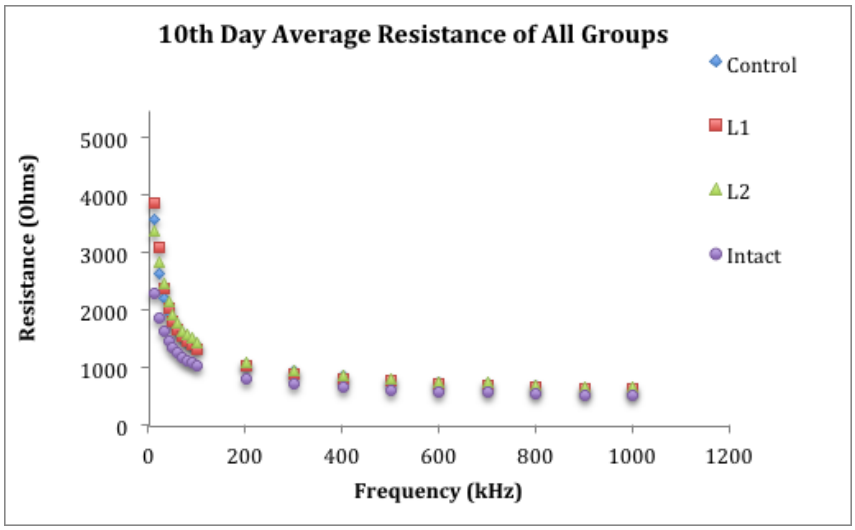

Figure 4.12 Electrical resistance values of control group, laser irradiation groups and intact skin samples from the lowest to the highest frequencies of measurement (10kHz - 1MHz) on the 10^{th} day of healing.

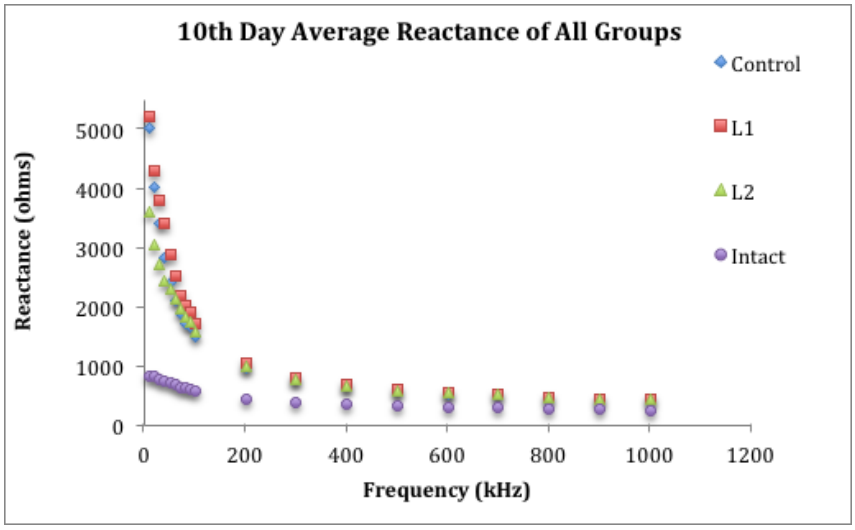

Figure 4.13 Electrical reactance values of control group, laser irradiation groups and intact skin samples from the lowest to the highest frequencies of measurement (10kHz - 1MHz) on the 10^{th} day of healing.

low and high frequency measurements are compared to the intact skin values as given in Figure 4.16.

4.3.2 COLE-COLE PLOTS

The Cole-Cole plots of each data set are first drawn separately. On the 3^{rd} day of healing, none of the experimental group wound samples have shown frequency dependent resistive and reactive properties that fit into Cole-Cole plot. Since wound areas for all

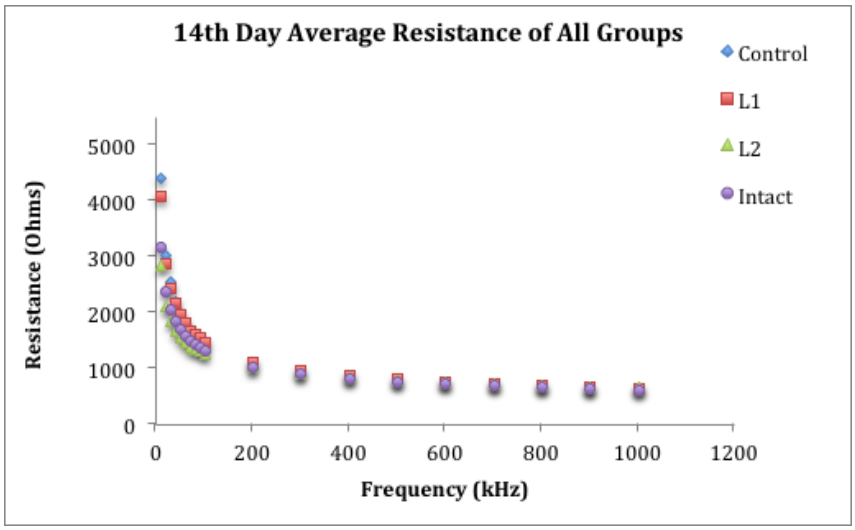

Figure 4.14 Electrical resistance values of control group, laser irradiation groups and intact skin samples from the lowest to the highest frequencies of measurement (10kHz - 1MHz) on the 14^{th} day of healing.

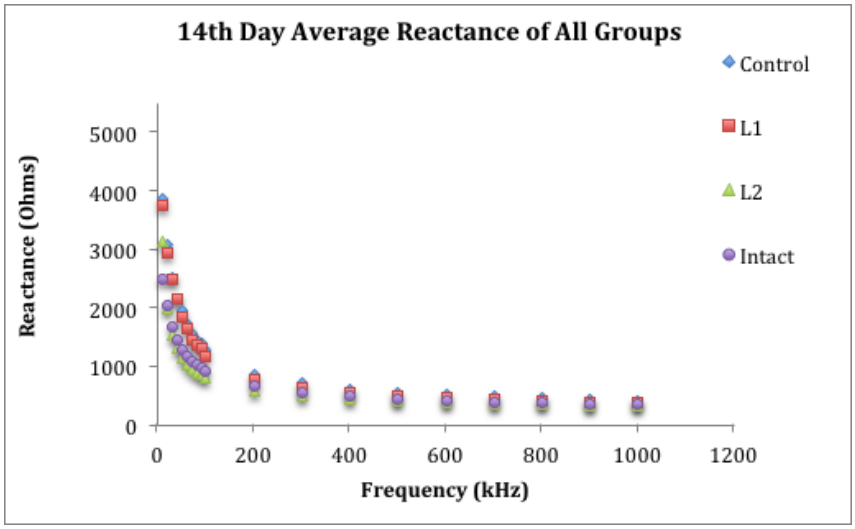

Figure 4.15 Electrical reactance values of control group, laser irradiation groups and intact skin samples from the lowest to the highest frequencies of measurement (10kHz - 1MHz) on the 14^{th} day of healing.

Table 4.3
Cole-Cole plot fit percentage of wound samples on each experiment day.

Group	3^{rd} Day	7^{th} Day	10^{th} Day	14^{th} Day
Intact	100	100	100	100
Control	0	50	50	75
1 J/cm^2	0	37.5	87.5	50
3 J/cm^2	0	62.5	75	37.5

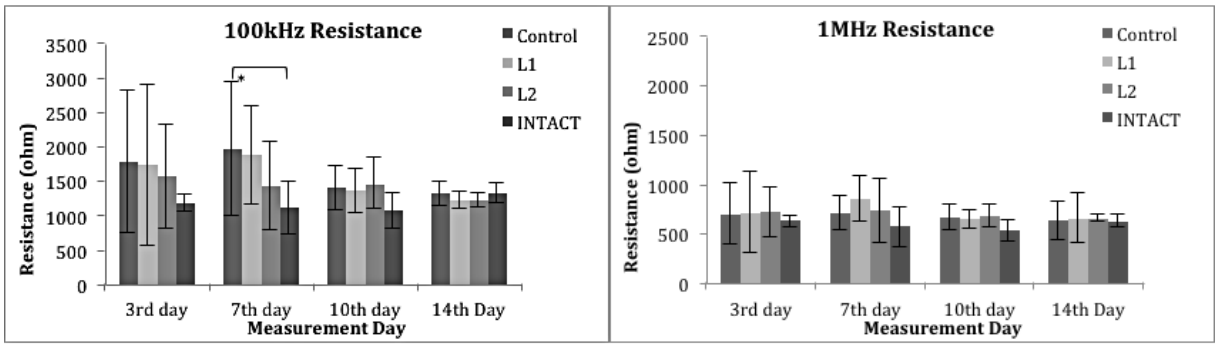

Figure 4.16 Average values of electrical resistance of each tissue sample at relatively low and high frequencies. Control group samples had higher resistance compared to laser treatment groups and intact skin for the 3^{rd} and 7^{th} days of healing. Following the 7^{th} day of healing resistance of both control group and laser group samples came close to that of healthy intact skin. On the 10^{th} and 14^{th} days, there was no remarkable difference between any of the groups and intact skin. Statistical evaluations were done using Kruskal-Wallis non-parametric test with a significance level of $p < 0.05$ (* indicates significance between groups).

tissues were still open with almost no signs of closure, this may have caused the electrical properties obtained not to fit into Cole-Cole model yet. However, it is observed that all of the impedance data collected across intact skin samples on separate measurement days fit the model without any exception (Figure 4.17).

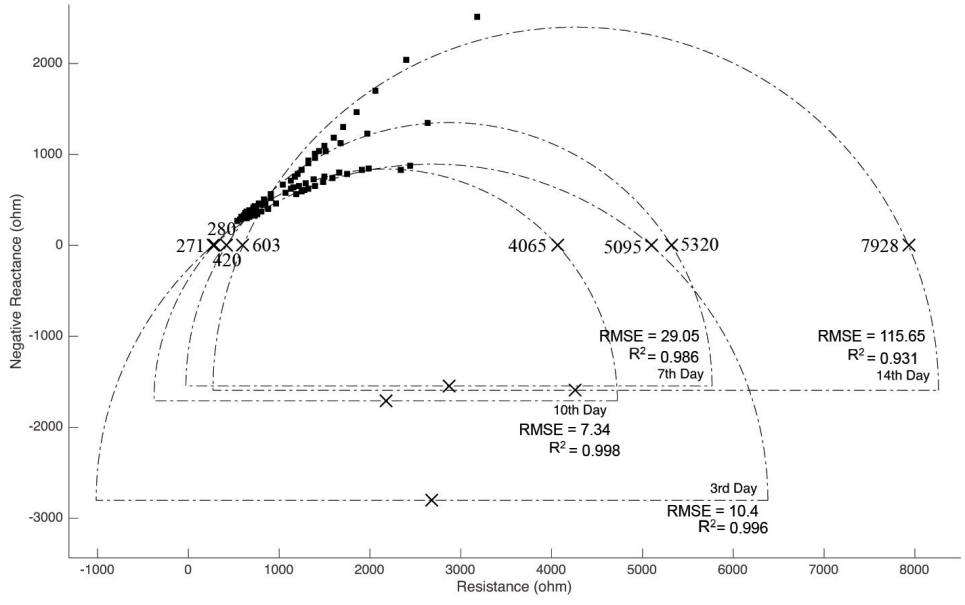

Figure 4.17 Cole-Cole diagrams of intact skin samples on the 3^{rd}, 7^{th}, 10^{th} and 14^{th} days of healing.

Although some of the results obtained on further measurement days that did not fit into the Cole-Cole model, it has been observed that the number of data sets obtained

from both control and laser irradiation group samples fitting into the Cole-Cole model have increased during the 7^{th}, 10^{th} and 14^{th} days of healing (Table 4.3).

4.4 HISTOLOGICAL EVALUATIONS

4.4.1 INCISIONAL WOUNDS

The histological examination results have shown that 635nm laser irradiation at 1 J/cm^2 and 3 J/cm^2 levels caused photobiomodulation on certain days of healing. However, 809nm laser stimulation did not show any positive effect on the healing process. Due to the results obtained from both in-vitro cell proliferation and in-vivo photobiomodulation experiments, excisional wounds were irradiated by means of only 635nm laser source of 1 J/cm^2 and 3 J/cm^2. Those results are given in the next chapter.

The incisional wounds including non-irradiated control group samples and laser treated wounds with both lasers of 635nm and 809nm wavelength were observed by eye inspection on the 3^{rd}, the 5^{th} and the 7^{th} days of healing in order to detect any deficiency or unexpected damage occurred. Samples, which have shown the signs of unexpected diseases at the wound site caused by physical disturbances, were excluded from the investigations.

On the 3^{rd} day of healing, all tissue samples have shown signs of degeneration with scar formation along the wound site. The control wounds have shown more prominent scar formation than laser treatment samples. Throughout the histological evaluations, laser groups and non-irradiated control samples were compared in terms of fibroblastic activity, collagen synthesis, neovascularization and degree of edema.

On the 3^{rd} of healing, 635nm laser irradiated tissues with both 1 and 3 J/cm^2 energy densities have shown better reepithelialization compared to the 809nm laser stimulated samples. In terms of fibroblastic activity and neovascularization, the samples of control and laser treatment groups of both wavelengths were not different from each other. On the other hand, collagen formation, which normally increases during the first days of the

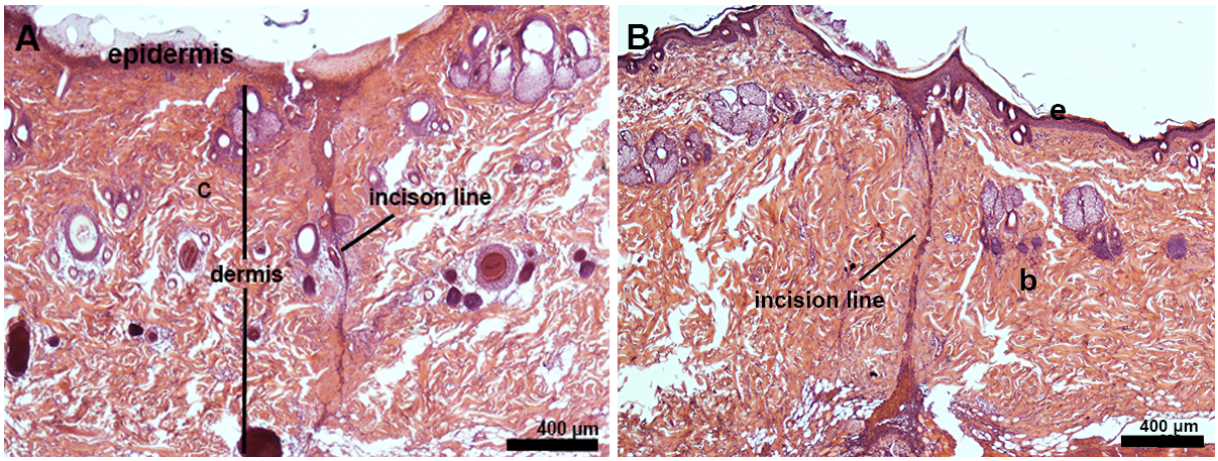

Figure 4.18 Hematoxylin and eosin stained incisional wound samples.

healing process, was remarkably higher for 635nm irradiated tissues compared to both control samples of both groups and 809nm laser irradiated tissues.

On the 5^{th} day of healing, 809nm laser irradiation of 1 J/cm^2 energy density have shown better signs of healing in terms of fibroblastic activity and vascularization. However, those differences were not significant to conclude that these two wavelengths had more or less biostimulation effect on the primary healing stages. Besides, when the two distinct wavelengths were compared in terms of collagen formation on the 5^{th} and 7^{th} days of healing, it is observed that 635nm laser irradiated tissues have shown higher degree of collagen formation due to higher amount of fibroblast proliferation.

4.4.2 EXCISIONAL WOUNDS

Excisional wounds were subjected to 635nm laser irradiations of 1 J/cm^2 and 3 J/cm^2 energy densities. Histological investigations were done by means of morphological examinations and semi-quantitative evaluations. The tissue samples excised on the 3^{rd}, 7^{th} and 10^{th} days of healing were morphologically examined. Wound surface areas (mm^2) of both laser irradiation groups were measured and compared with the average of control group tissues. It has been observed that on the 14^{th} day of healing, all of the wounds were completely closed. On the 3^{rd} day of healing, both laser treated samples had smaller

wound areas compared to the control group samples. However, those differences were not significantly different from each other according to statistical analysis. On the other hand, the 7^{th} day measurements show significant amount of wound closure for 3 J/cm^2 samples with respect to the control group tissues. There were no statistically important change in the wound sizes of 1 J/cm^2 group samples compared to both control and 3 J/cm^2 groups. Similar results were obtained on the 10^{th} day of examinations at which 3 J/cm^2 group wounds were diminished significantly in terms of area compared to both control and 1 J/cm^2 group tissues.

Table 4.4
Average wound areas (a,b indicating significant difference compared to the control group).

Day	Group	Mean Area±SD (mm^2)
	Control	57.83 ± 11.05^a
3^{rd} Day	1 J/cm^2	51.33 ± 8.15^a
	3 J/cm^2	50.65 ± 4.73^a
	Control	21.02 ± 1.47^a
7^{th} Day	1 J/cm^2	15.24 ± 1.78^a
	3 J/cm^2	13.89 ± 1.73^b
	Control	0.90 ± 0.35^a
10^{th} Day	1 J/cm^2	1.07 ± 0.34^a
	3 J/cm^2	1.33 ± 0.19^b

4.4.2.1 Semi-quantitative Evaluations. On the 3^{rd} day of healing, tissues observed at all groups have shown incomplete and irregular reepithelialization with epithelial disintegration and blot clot formation, which is not only a dynamic matrix of proteins but it also serves as a provisional lattice for incoming inflammatory cells, fibroblasts and several growth factors [3]. On the 3^{rd} day of healing, results showed significantly higher fibroblastic activity for both laser irradiation groups compared to the control wounds. However, the laser groups were not different from each other. It is observed that tissues exposed to 3 J/cm^2 laser irradiation had significantly higher blood vessels than that of the 1 J/cm^2 laser treated samples. The collagen synthesis of 1 J/cm^2 laser irradiated tissues

was significantly lower than both 3 J/cm^2 laser samples and non-irradiated control tissues (Figure 4.19). On the 7^{th} day of healing, scab formation with moderate keratinization of prominently thicker epidermis was observed on control wounds compared to both laser groups. Fibroblastic activity after the 3^{rd} day is observed to decrease for 3 J/cm^2 laser treatment group. However, control group samples and 1 J/cm^2 laser irradiated tissues had remarkable amount of increased fibroblastic activity. During the first days of healing, small amount of blood vessels was observed in control group and 1 J/cm^2 group tissues. On the 3^{rd} day, 3 J/cm^2 group tissues had significantly higher amount of vessels compared to the 1 J/cm^2 laser samples. But then, it is found to increase following the progress of healing. This increase was especially remarkable for 1 J/cm^2 group samples between the 3^{rd} and 7^{th} days of healing. Although there were variations in the amount of collagen synthesis until the end of the acute inflammation phase especially in the control group samples, all tissue samples had similar quantities of collagen synthesis during the maturation phase of healing (Figure 4.20).

On day 10 following irradiations, all tissue samples had signs of improvement in terms of healing. It is observed that epidermal thicknesses of all samples were decreased due to scab detachment above the epidermis. On 14^{th} day of the study, all wound samples were almost totally closed. The alterations in the wound healing parameters were not different anymore between the control and laser treatment group samples. Keratinization along the epidermal surface was completed with very slight presence of crust. Granulation tissue through the dermis had significant amount of newly formed collagen for each sample with no remarkable difference between groups.

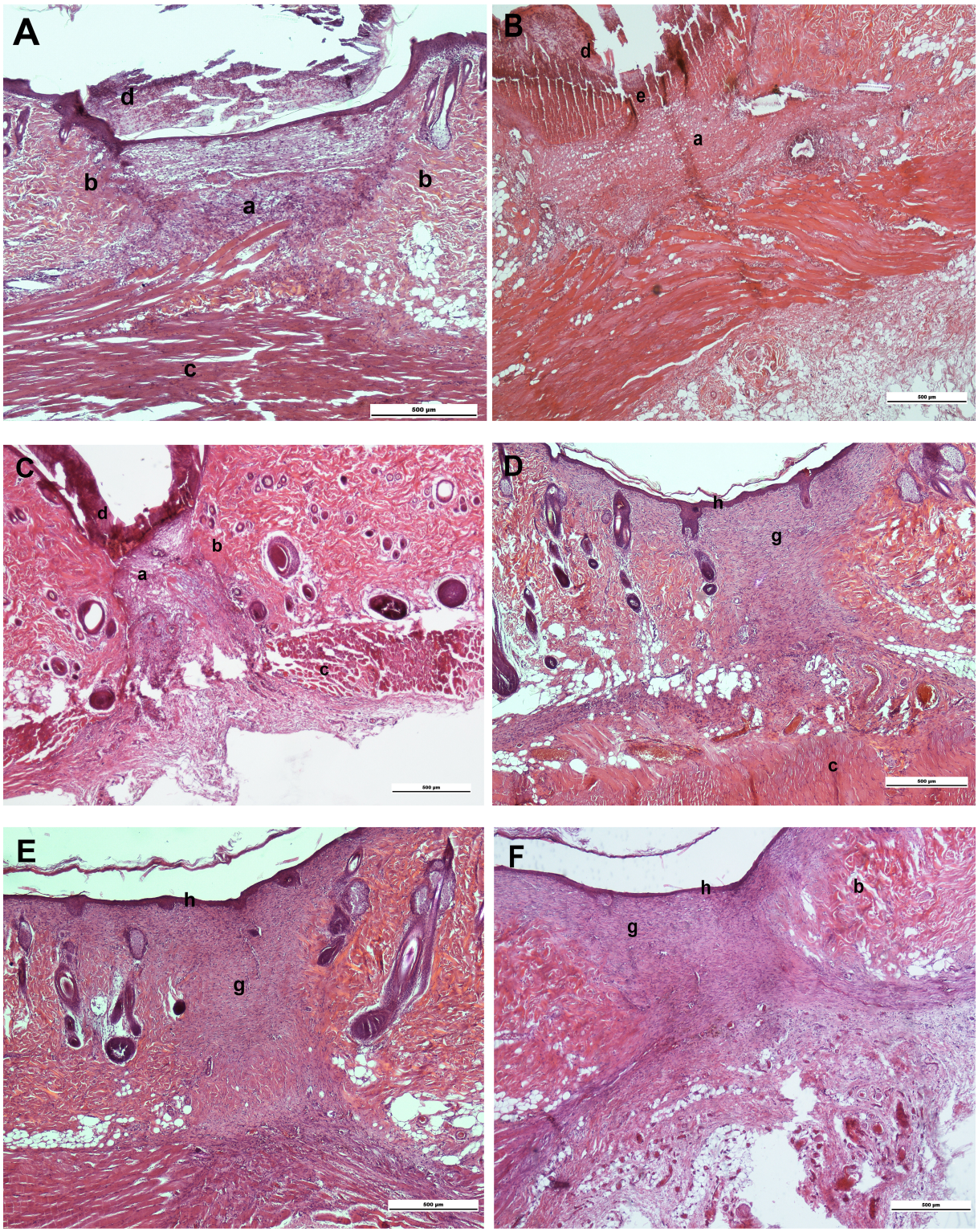

Figure 4.19 Hematoxylin and eosin stained tissue samples on 3^{rd} day and 14^{th} days of healing. A Day 3 - Control (a Early granulation tissue, b Healthy peripheral tissue, c Dense collagenous fascia tissue, d Scab formation). B Day 3 - L1 group (a Early granulation tissue, e Incomplete reepithelialization, d Scab formation). C Day 3 - L2 group (a Granulation tissue, b Healthy peripheral tissue, c Dense collagenous fascia and striated muscle, d Scab formation). D Day 14 - Control (g Early scar tissue with higher amount of collagen, h Reepithelialization, c Dense collagenous fascia tissue). E Day 14 - L1 (g Early scar tissue, h Reepithelialization). F Day 14 - L2 (g Early scar tissue, b Healthy peripheral tissue, h Reepithelialization). Scale bars represent 500 μm.

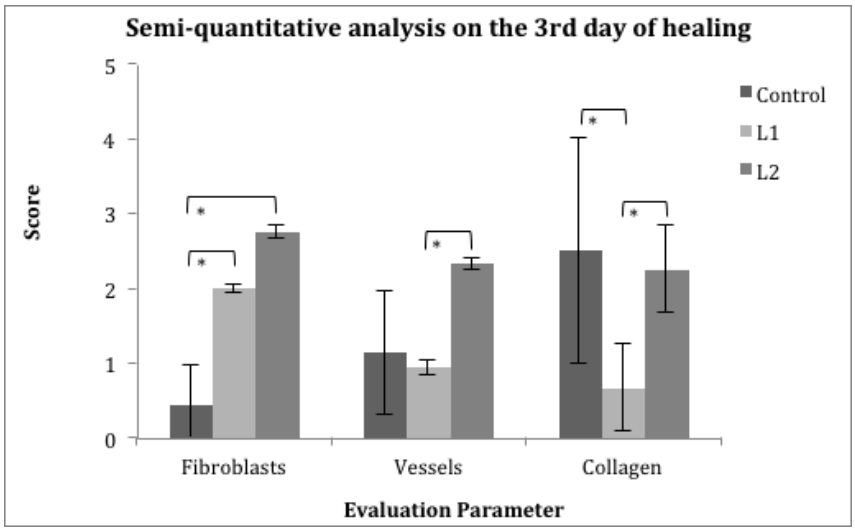

Figure 4.20 Semi-quantitative evaluation of histological examinations on the 3^{rd} day of healing. Statistical evaluations were done Analysis of Variance (ANOVA) with a significance level of $p < 0.05$ (* indicates significance between groups).

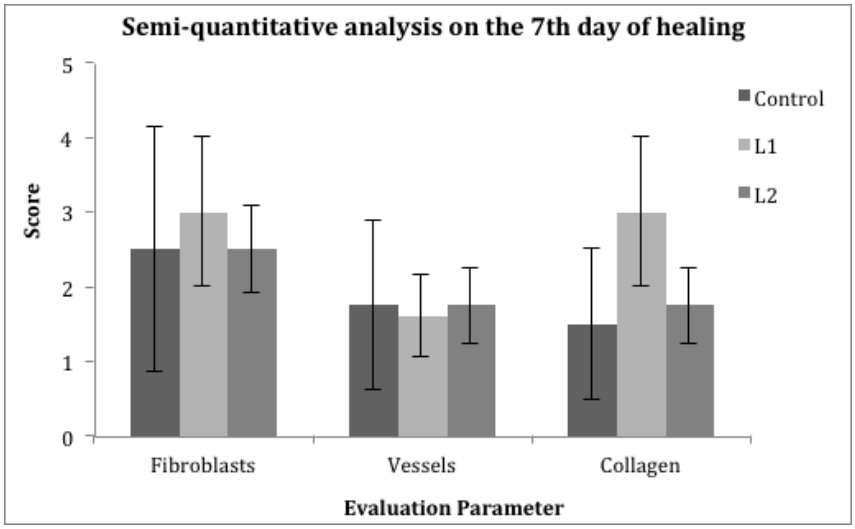

Figure 4.21 Semi-quantitative evaluation of histological examinations on the 7^{th} day of healing. Statistical evaluations were done Analysis of Variance (ANOVA) with a significance level of $p < 0.05$ (* indicates significance between groups).

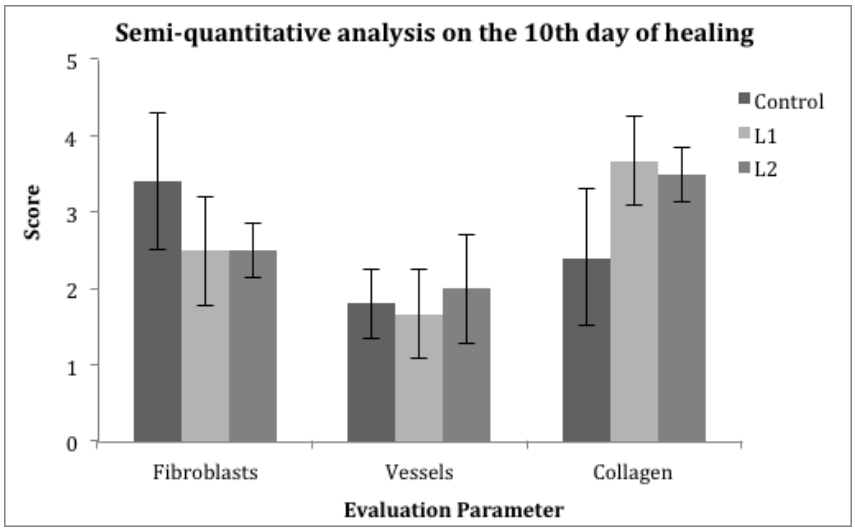

Figure 4.22 Semi-quantitative evaluation of histological examinations on the 10^{th} day of healing. Statistical evaluations were done Analysis of Variance (ANOVA) with a significance level of $p < 0.05$ (* indicates significance between groups).

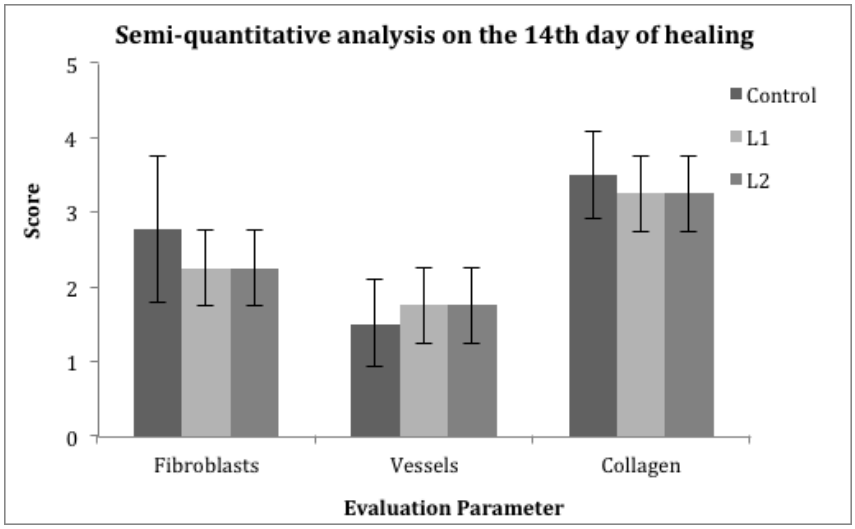

Figure 4.23 Semi-quantitative evaluation of histological examinations on the 14^{th} day of healing. Statistical evaluations were done Analysis of Variance (ANOVA) with a significance level of $p < 0.05$ (* indicates significance between groups).

5. DISCUSSIONS AND CONCLUSSION

Wound healing is a continuous and dynamic process of many molecular, cellular and biochemical events occurring simultaneously [76]. Normal healing begins immediately after the injury due to the triggering of platelets to release of clotting factors and cytokines [30]. The three basic mechanisms that occur during normal healing of dermal wounds are epithelialization, connective tissue deposition and tissue contraction. Wounds, which are closed by staples or sutures, heal by Primary Intention. During this process, fibroblast proliferation has critical importance due to the amount of connective tissue deposition. On the contrary, wounds that remain open during the healing heal by Secondary Intention. Secondary Intention is due to contraction of the wound, at which cells and extracellular matrix around the wound site move through the center of the wound. Wound contraction occurs manly because of the interaction between myofibroblasts and matrix components [30].

Laser photobiomodulation (PBM) on wound healing has recently been one of the most interesting subjects due to its importance on understanding the alterations of events and mechanisms during wound healing process. It is a very easy to apply, repeatable and highly safe treatment method once the optimal parameters are chosen with no risk of bacterial infection. There are many studies in literature reporting the positive (75%), negative and no-effect (25%) results of laser photobiomodulation in-vitro and in-vivo. Recently almost 20% of the biostimulation research used cell cultures, whereas about 80% of those studies used animal subjects as target. Out of these percentages, more than 87% of the animals used during the experiments were rats. The most commonly used laser wavelengths are 632.5nm in the short and 904nm in the long wavelengths with varying energy densities between 0.1-140 J/cm^2. Hawkins et al. [94] reported that visible red and near infrared wavelengths of the light spectrum have unique therapeutic effects on tissues due to relatively higher absorption [95]. Out of this wide range, 1-4 J/cm^2 has been the most frequently used energy dose [60]. Therefore, it is not only the in-vivo wound models on animal subjects, which helps understanding the mechanisms behind the complicated

process of wound healing, but it also is important to examine the cell behaviour in the in-vitro laboratory conditions.

It is known that photobiomodulation can stimulate various cellular processes, such as cell growth, cell proliferation and differentiation. Even though there are many reports regarding the in-vitro effects of laser biostimulation in various cell types (fibroblasts, endothelial cells, skeletal cells and keratinocytes and etc.), the overall mechanism has not been fully understood yet [68,70]. Cell viability and proliferation are critically important physiological signs for examining the biostimulation effect of photobiomodulation [96, 97]. Fibroblasts as being one of the most important cells migrate to the wound site during the beginning of proliferation phase and have got many functions. They synthesize the extracellular matrix collagen found in the connective tissue and are responsible for the production of several cytokines and growth factors. Using cell culture models is advantageous since it provides a controlled environment to study a wide variety of cellular phenomena [98] however, it may also have some limitations regarding isolation of cells from the supplementary elements in-vivo. But it is crucially important to investigate the in-vitro effects of biostimulation for improving the current understanding of mechanisms of growth, differentiation and development of cells [99]. It was proposed that low-level laser therapy promoted human gingival fibroblast biostimulation in-vitro by means of 809nm diode laser application [99]. Basso et al reported that laser biostimulation of 780nm wavelength at 0.5 and 3 J/cm^2 energy densities resulted in significant increase in cell metabolism [74]. However, same group promoted non-significant changes for the total protein production of keratinocytes induced by means of same laser sources [73]. On the other and, Güngörmüş et al suggested that laser irradiation schedule is more important than the total energy dose of the treatment [100]. The relative absorption values obtained from the results of MTT analysis of our study showed that 635nm laser irradiation of both 1 J/cm^2 and 3 J/cm^2 energy densities caused increased cell viability during the first 24 hours of the examinations. However, 809 nm laser irradiation did not have any positive or negative effect on cell viability during the first 48 hours of examinations.

In-vivo wound healing was examined under mechanical tensile tests, histological examinations and electrical bioimpedance measurements. Tensile strength of skin tissue is

a parameter used for describing the condition of the sample. As already mentioned earlier, fibroblast is the most common type of cell found in the connective tissue, which is responsible for synthesizing the extracellular matrix and collagen during the proliferation phase of healing and has critical role in terms of wound strength. It is known that collagen deposition is effective in increasing wound strength [95,101]. Once fibroblasts are activated, they differentiate into myofibroblasts that participate in secretion of extracellular matrix proteins and have role in reducing the wound size by contraction. Chronic wounds with deficient or incomplete healing suffer from adequate collagen production, which changes the mechanical strength of tissues. Riou et.al reported that tensile strength of diabetic wounds was lower than that of non-diabetic wounds. Hence, the total collagen content of injured tissues is claimed to be directly proportional to the tensile strength [101]. The findings from the our study indicated that breaking strength of incisional wounds exposed to 635nm laser irradiation of 1 J/cm^2 was found to significantly increase until the 5^{th} day of healing compared to control group results. Similarly, 3 J/cm^2 energy density of 635nm laser exposure increased the tensile strength values of wound samples on the 7^{th} day of healing. However, 809nm laser irradiation at both energy densities did not have any stimulative effect on tensile strength of incisional samples. The increase in tensile strength is related to the increase in collagen deposition in the dermis. Although there are many conflicting results reported in literature about the tensile strength of incisions [102–104], our examinations showed the biostimulation effects of 635nm laser irradiation of low energy densities consistent with many other studies [95, 105, 106].

Following the mechanical tensile strength tests, morphological and histological examinations were performed on incisional and excisional cutaneous skin wounds on the 3^{rd}, 7^{th}, 10^{th} and 14^{th} days of healing. Morphological investigations showed that both energy densities of 635nm laser irradiation had positive effects on wound closure. On the 3^{rd} day of healing, both incisional and excisional samples exposed to 635nm laser-irradiation showed better signs of reepithelialization compared to non-irradiated control group and 809nm irradiation tissues. The incisional wounds during the healing process did not have a remarkable difference between groups in terms of fibroblast activity and blood vessel formation for both wavelengths. Based on the findings on incisions, excisional samples exposed to 635nm laser were compared morphologically and histologically. Samples exposed

to both energy densities had smaller surface areas than control group samples on the 3^{rd} and 7^{th} days of healing. It has been observed that all groups had apparent blood clot formation followed by vasoconstriction and incomplete reepithelialization, which are the two dominating events occurring during the first days of healing, namely inflammation phase. However, control group tissues had a thicker outmost layer surrounded with higher amount of scar tissue. After 10^{th} day of healing, the morphological alterations between groups were not considerably different from each other. In addition, tissue samples compared histologically with the semi-quantitative evaluations of fibroblast activity, collagen synthesis and the rate of newly formed blood vessels on 3^{rd}, 7^{th}, 10^{th} and 14^{th} days of healing. As already given in the results section, the semi-quantitative evaluations showed that 635nm laser irradiation of both 1 and 3 J/cm^2 energy densities had positive affects on the healing process for the first days of healing in terms of fibroblast activity and angiogenesis. Many other parameters such as reepithelialization, scar tissue formation, epidermal thickness and content of the dermis were also found to be consistent with the semi-quantitative evaluations.

Finally, changes in the electrical conductivity of excisional wounds were investigated by means of multi-frequency complex electrical impedance measurements. Measurements of resistance and capacitance of living tissue reflects the changes in the electrical properties of extracellular fluid and electrolyte composition and cell membrane mass and function respectively [15].

Electrical impedance of living tissues is generally examined in three main frequency regions with decreasing impedance values with increasing frequency. These regions correspond to specific molecular and cellular events. The α-dispersion (mHz - few kHz) reflects the polarization of ions near the membrane surfaces. This region has usually been under the focus of impedance measurements of living tissues. The β-dispersion (few kHz - hundreds of MHz) reflects the structural changes of the cell membranes and edema. The γ-dispersion (hundreds of MHz - several GHz) on the other hand is related to the relaxation of polar molecules such as water. Ackmann and Seits showed the relation between the electrical impedance of intact skin and the outermost layer of skin, namely stratum corneum (SC) at frequencies lower than 1kHz and higher than 1MHz [107]. This was

confirmed by the computational study of Martinsen et al [108]. Birgersson et al showed that the electrical impedance of intact skin is strongly dominated by stratum corneum up to frequencies of even 1MHz [109]. During the inflammation phase of healing on the very first days post-irradiation, blood clot formation following the vasoconstriction causes the blood flow to decrease through the wound site. The reduced water concentration at the wound area may cause the electrical resistance of wounded tissues to be greater than the intact skin resistance at these first days of healing. The effect of varying water content on skin membrane resistance was reported previously [110]. In our study, similar results consistent with the findings in literature were obtained at each frequency of impedance measurements. Our results obtained specifically at frequencies higher than 100 kHz showed that the resistance values of laser treated wounds were very close to that of the intact skin. This may be due to many metabolic and cellular events, such as the differences between thickness and continuity of the newly formed layers and structures of the wound tissues or the amount of growth factors released at the wound site that causes the migration of fibroblasts and neutrophils through the target tissue. The increase in resistance values is directly proportional to the decreased extracellular fluid, increased cell mass and reepithelialization [15].

In our study resistance of all tissue samples of the three experimental groups increased until day 7 and then decreases back until 10^{th} day. On the 7^{th} day of healing, we observed that scab formation along epidermis on both control group and laser treatment groups may have resulted with an increase in the electrical resistance of tissues during the proliferation of healing process. Electrical resistance, which is directly proportional to cell mass, epidermal proliferation and thickness of subcutaneous fat layer and inversely related to the extracellular fluid concentration, is also strongly related to the thickness of the newly formed stratum corneum (SC) layer dominating the resistance of tissues in the frequency range of measurements. The higher values of resistance obtained from laser irradiated wounds with more coordinated SC layer in our study supports the previously reported findings [107, 108, 111]. This is similar to the findings of many previous reports suggesting that the thickness and continuity of SC is directly proportional to the resistance of tissues [15, 111]. Along with the presence of scar tissue formation, continuity of upper epidermis may cause the resistance values to increase until 7^{th} day of healing. 10^{th} day

measurement results show that control and laser irradiation tissues have resistance and reactance values very close to each other at every frequency of measurement. Following the 10^{th} day, resistance of the control group and 1 J/cm^2 laser treatment group samples further increased until complete epithelialization was reached, which was observed in all wound samples on the 14^{th} day as an indicator of completed healing.

Capacitive response of the tissues caused by the lipid bilayer cell membrane is suggested to be directly proportional to the cell mass. Increase in the capacitive reactance may sign to an increased formation of granulation tissue and epidermal proliferation. It has been observed that, reactance of wound samples for all groups increased until 7^{th} day examinations similar to the changes of resistance values. Thus, it may be suggested according to this study that it is not only the resistance but also the capacitive reactance of tissues, which are directly proportional to the cell mass, epidermal proliferation and continuity of subcutaneous fat layer and inversely proportional to the extracellular fluid. Therefore, it may be finally concluded that higher the complex impedance of tissues, better the progress of healing process. In our study, 1 J/cm^2 laser irradiated wounds having the greatest resistance at almost every frequency, especially at frequencies higher than 100 kHz, shows signs of improved healing compared to other groups. We may suggest that the electrical impedance values obtained support the histological findings for the first seven days of healing. Research on wound healing had many examples of consistent changes of electrical impedance parameters in various wound models. Keese et al. showed the direct relationship between the electrical resistance values of a cell culture model with the growth of a functional monolayer [112]. Resistance increased significantly during the growth, whereas decreased after the disruption of the layer. Their finding is considered to be a good sign of evidence that electrical resistance is a good indicator of cell growth during the healing process. Spence et al. monitored the change in transcutaneous electrical resistance during the healing of surgically induced wounds in rodents. Results showed that resistance values decreased significantly after skin incisions and increased back during a healing period of 20 days [111]. Phase-sensitive impedance measurements performed on adult subjects at different levels of risk for pressure ulcers have shown that patients higher risk for ulcers had significantly lower resistance and capacitive reactance values compared to control croup samples. Wagner et al. suggested that those results

were the indicators of malnutrition, extracellular fluid accumulation and reduced cellular vitality. Besides, capacitive reactance (X_C) as being an important predictor of risk for pressure ulcers with a coefficient of determination of 0.96, is also an indicator of cell mass [75, 108].

Although there are many interventions and methods for monitoring the complicated process of healing, most of them are strongly affected by the subjective decisions of the researchers and have limitations such as reliability and repeatability, accuracy and time efficiency [75, 95, 98]. The need of an objective method that may reveal reliable results that may indicate physiological and biochemical changes during the healing is crucial. Thus, electrical bioimpedance measurements may be used as a supporting method to conventional histological and mechanical examinations for monitoring the healing process.

REFERENCES

1. Gulsoy, M., Z. Dereli, H. O. Tabakoglu, and O. Bozkulak, "Closure of skin incisions by 980-nm diode laser welding," *Lasers in Medical Science*, Vol. 21, no. 1, pp. 5–10, 2006.

2. Lazarus, G. S., D. M. Cooper, D. R. Knighton, D. J. Margolis, R. E. Percoraro, G. Rodeheaver, and M. C. Robson, "Definitions and guidelines for assessment of wounds and evaluation of healing," *Wound Repair and Regeneration*, Vol. 2, no. 3, pp. 165–170, 1994.

3. Karu, T., "Primary and secondary mechanisms of action of visible to near-ir radiation on cells," *Journal of Photochemistry and photobiology B: Biology*, Vol. 49, no. 1, pp. 1–17, 1999.

4. Karu, T., "Photobiology of low-power laser effects.," *Health physics*, Vol. 56, no. 5, pp. 691–704, 1989.

5. Karu, T. I., "Effects of visible radiation on cultured cells," *Photochemistry and photobiology*, Vol. 52, no. 6, pp. 1089–1098, 1990.

6. Karu, T. I., "Low-power laser therapy," *Biomedical photonics handbook*, Vol. 48, pp. 1–25, 2003.

7. Wong-Riley, M. T., H. L. Liang, J. T. Eells, B. Chance, M. M. Henry, E. Buchmann, M. Kane, and H. T. Whelan, "Photobiomodulation directly benefits primary neurons functionally inactivated by toxins role of cytochrome c oxidase," *Journal of Biological Chemistry*, Vol. 280, no. 6, pp. 4761–4771, 2005.

8. Pastore, D., M. Greco, V. Petragallo, and S. Passarella, "Increase in h+/e-ratio of the cytochrome c oxidase reaction in mitochondria irradiated with helium-neon laser.," *Biochemistry and molecular biology international*, Vol. 34, no. 4, pp. 817–826, 1994.

9. Karu, T., L. Pyatibrat, and G. Kalendo, "Irradiation with he-ne laser increases atp level in cells cultivated in vitro," *Journal of Photochemistry and photobiology B: Biology*, Vol. 27, no. 3, pp. 219–223, 1995.

10. Harris, D. M., "Editorial comment biomolecular mechanisms of laser biostimulation," *Journal of clinical laser medicine & surgery*, Vol. 9, no. 4, pp. 277–280, 1991.

11. Avci, P., A. Gupta, M. Sadasivam, D. Vecchio, Z. Pam, N. Pam, and M. R. Hamblin, "Low-level laser (light) therapy (lllt) in skin: stimulating, healing, restoring," in *Seminars in cutaneous medicine and surgery*, Vol. 32, pp. 41–52, Frontline Medical Communications, 2013.

12. Gupta, A., P. Avci, M. Sadasivam, R. Chandran, N. Parizotto, D. Vecchio, W. C. de Melo, T. Dai, L. Y. Chiang, and M. R. Hamblin, "Shining light on nanotechnology to help repair and regeneration," *Biotechnology advances*, Vol. 31, no. 5, pp. 607–631, 2013.

13. Karu, T., and S. Kolyakov, "Exact action spectra for cellular responses relevant to phototherapy," *Photomedicine and Laser Therapy*, Vol. 23, no. 4, pp. 355–361, 2005.

14. Greco, M., G. Guida, E. Perlino, E. Marra, and E. Quagliariello, "Increase in rna and protein synthesis by mitochondria irradiated with helium-neon laser," *Biochemical and biophysical research communications*, Vol. 163, no. 3, pp. 1428–1434, 1989.

15. Lukaski, H. C., and M. Moore, "Bioelectrical impedance assessment of wound healing," *Journal of diabetes science and technology*, Vol. 6, no. 1, pp. 209–212, 2012.

16. Dean, D., T. Ramanathan, D. Machado, and R. Sundararajan, "Electrical impedance spectroscopy study of biological tissues," *Journal of electrostatics*, Vol. 66, no. 3, pp. 165–177, 2008.

17. McRae, D. A., M. A. Esrick, and S. C. Mueller, "Changes in the noninvasive, in vivo electrical impedance of three xenografts during the necrotic cell-response sequence," *International Journal of Radiation Oncology* Biology* Physics*, Vol. 43, no. 4, pp. 849–857, 1999.

18. Soley, A., M. Lecina, X. Gamez, J. Cairo, P. Riu, X. Rosell, R. Bragos, and F. Godia, "Online monitoring of yeast cell growth by impedance spectroscopy," *Journal of biotechnology*, Vol. 118, no. 4, pp. 398–405, 2005.

19. Solmaz, H., Y. Ülgen, and M. Tümer, "Design of a microcontroller based cole-cole impedance meter for testing biological tissues," in *World Congress on Medical Physics and Biomedical Engineering, September 7-12, 2009, Munich, Germany*, pp. 488–491, Springer, 2009.

20. Yang, Y., J. Wang, G. Yu, F. Niu, and P. He, "Design and preliminary evaluation of a portable device for the measurement of bioimpedance spectroscopy," *Physiological Measurement*, Vol. 27, no. 12, p. 1293, 2006.

21. Kyle, U. G., I. Bosaeus, A. D. De Lorenzo, P. Deurenberg, M. Elia, J. M. Gómez, B. L. Heitmann, L. Kent-Smith, J.-C. Melchior, M. Pirlich, *et al.*, "Bioelectrical impedance analysis—part i: review of principles and methods," *Clinical nutrition*, Vol. 23, no. 5, pp. 1226–1243, 2004.

22. Ngawhirunpat, T., T. Hatanaka, K. Katayama, H. Yoshikawa, J. Kawakami, and I. Adachi, "Changes in electrophysiological properties of rat skin with age.," *Biological and Pharmaceutical Bulletin*, Vol. 25, no. 9, pp. 1192–1196, 2002.

23. Kun, S., B. Ristic, R. A. Peura, and R. M. Dunn, "Algorithm for tissue ischemia estimation based on electrical impedance spectroscopy," *IEEE transactions on biomedical engineering*, Vol. 50, no. 12, pp. 1352–1359, 2003.

24. Mayer, M., P. Brunner, R. Merwa, and H. Scharfetter, "Monitoring of lung edema using focused impedance spectroscopy: a feasibility study," *Physiological measurement*, Vol. 26, no. 3, p. 185, 2005.

25. Aberg, P., I. Nicander, J. Hansson, P. Geladi, U. Holmgren, and S. Ollmar, "Skin cancer identification using multifrequency electrical impedance-a potential screening tool," *IEEE Transactions on Biomedical Engineering*, Vol. 51, no. 12, pp. 2097–2102, 2004.

26. Robson, M. C., D. L. Steed, and M. G. Franz, "Wound healing: biologic features and approaches to maximize healing trajectories," *Current problems in surgery*, Vol. 38, no. 2, pp. 72–140, 2001.

27. Baum, C. L., and C. J. Arpey, "Normal cutaneous wound healing: clinical correlation with cellular and molecular events," *Dermatologic surgery*, Vol. 31, no. 6, pp. 674–686, 2005.

28. Becker, B., B. Heindl, C. Kupatt, and S. Zahler, "Endothelial function and hemostasis," *Zeitschrift für Kardiologie*, Vol. 89, no. 3, pp. 160–167, 2000.

29. Lawrence, W. T., "Physiology of the acute wound.," *Clinics in plastic surgery*, Vol. 25, no. 3, pp. 321–340, 1998.

30. Diegelmann, R. F., and M. C. Evans, "Wound healing: an overview of acute, fibrotic and delayed healing," *Front Biosci*, Vol. 9, no. 1, pp. 283–289, 2004.

31. Monaco, J. L., and W. T. Lawrence, "Acute wound healing: an overview," *Clinics in plastic surgery*, Vol. 30, no. 1, pp. 1–12, 2003.

32. RO, H., "Fibronectins," *Sci Am.*, Vol. 254, no. 6, pp. 42–51, 1986.

33. Deuel, T. F., R. M. Senior, J. Huang, and G. Griffin, "Chemotaxis of monocytes and neutrophils to platelet-derived growth factor.," *Journal of Clinical Investigation*, Vol. 69, no. 4, p. 1046, 1982.

34. Clark, R. A., J. M. Lanigan, P. DellaPelle, E. Manseau, H. F. Dvorak, and R. B. Colvin, "Fibronectin and fibrin provide a provisional matrix for epidermal cell migration during wound reepithelialization," *Journal of Investigative Dermatology*, Vol. 79, no. 5, pp. 264–269, 1982.

35. Wysocki, A., and F. Grinnell, "Fibronectin profiles in normal and chronic wound fluid.," *Laboratory investigation; a journal of technical methods and pathology*, Vol. 63, no. 6, pp. 825–831, 1990.

36. Cohen IK, Diegelman RF, D. R. e. a., "Wound healing: In: Greenfield lj, mulholland mw, oldham kt, et al, editors.," *Surgery: scientific principles and practice. third edition*, 1993.

37. Werner, S., and R. Grose, "Regulation of wound healing by growth factors and cytokines," *Physiological reviews*, Vol. 83, no. 3, pp. 835–870, 2003.

38. Majno, G., S. M. Shea, and M. Leventhal, "Endothelial contraction induced by histamine-type mediators an electron microscopic study," *The Journal of cell biology*, Vol. 42, no. 3, pp. 647–672, 1969.

39. Velnar, T., T. Bailey, and V. Smrkolj, "The wound healing process: an overview of the cellular and molecular mechanisms," *Journal of International Medical Research*, Vol. 37, no. 5, pp. 1528–1542, 2009.

40. Hart, J., "Inflammation. 1: Its role in the healing of acute wounds.," *Journal of wound care*, Vol. 11, no. 6, pp. 205–209, 2002.

41. Hunt, T. K., "The physiology of wound healing," *Annals of emergency medicine*, Vol. 17, no. 12, pp. 1265–1273, 1988.

42. Sieggreen, M., "Healing of physical wounds.," *The Nursing clinics of North America*, Vol. 22, no. 2, pp. 439–447, 1987.

43. Postlethwaite, A. E., J. Keski-Oja, G. Balian, and A. Kang, "Induction of fibroblast chemotaxis by fibronectin. localization of the chemotactic region to a 140,000-molecular weight non-gelatin-binding fragment.," *The Journal of experimental medicine*, Vol. 153, no. 2, pp. 494–499, 1981.

44. Gallo, R. L., "Proteoglycans and cutaneous vascular defense and repair," in *Journal of Investigative Dermatology Symposium Proceedings*, Vol. 5, pp. 55–60, Elsevier, 2000.

45. Remensnyder, J., and G. Majno, "Oxygen gradients in healing wounds.," *The American journal of pathology*, Vol. 52, no. 2, p. 301, 1968.

46. Thurston, G., C. Suri, K. Smith, J. McClain, T. Sato, G. Yancopoulos, and D. McDonald, "Leakage-resistant blood vessels in mice transgenically overexpressing angiopoietin-1," *Science*, Vol. 286, no. 5449, pp. 2511–2514, 1999.

47. Beck, E., "The influence of fibrin-stabilizing factor on the growth of fibroblasts in vitro and wound healing," *Thromb Diath Haemorrh*, Vol. 6, pp. 485–491, 1961.

48. Coulombe, P. A., "Wound epithelialization: Accelerationg the pace of discovery," *Journal of Investigative Dermatology*, Vol. 121, no. 2, pp. 219–230, 2003.

49. Grzesiak, J. J., and M. D. Pierschbacher, "Shifts in the concentrations of magnesium and calcium in early porcine and rat wound fluids activate the cell migratory response.," *Journal of Clinical Investigation*, Vol. 95, no. 1, p. 227, 1995.

50. Daniel, R. J., and R. W. Groves, "Increased migration of murine keratinocytes under hypoxia is mediated by induction of urokinase plasminogen activator," *Journal of investigative dermatology*, Vol. 119, no. 6, pp. 1304–1309, 2002.

51. Bullard, K. M., L. Lund, J. S. Mudgett, T. N. Mellin, T. K. Hunt, B. Murphy, J. Ronan, Z. Werb, and M. J. Banda, "Impaired wound contraction in stromelysin-1–deficient mice," *Annals of surgery*, Vol. 230, no. 2, p. 260, 1999.

52. Nimni, M. E., "Collagen: its structure and function in normal and pathological connective tissues," in *Seminars in arthritis and rheumatism*, Vol. 4, pp. 95–150, WB Saunders, 1975.

53. Ignotz, R. A., and J. Massague, "Transforming growth factor-beta stimulates the expression of fibronectin and collagen and their incorporation into the extracellular matrix.," *Journal of Biological Chemistry*, Vol. 261, no. 9, pp. 4337–4345, 1986.

54. Gabbiani, G., G. Ryan, and G. Majno, "Presence of modified fibroblasts in granulation tissue and their possible role in wound contraction," *Experientia*, Vol. 27, no. 5, pp. 549–550, 1971.

55. Ehrlich, H. P., "The role of connective tissue matrix in wound healing.," *Progress in clinical and biological research*, Vol. 266, pp. 243–258, 1987.

56. Clark, R. A., "Regulation of fibroplasia in cutaneous wound repair.," *The American journal of the medical sciences*, Vol. 306, no. 1, pp. 42–48, 1993.

57. Falanga, V., "Wound healing and chronic wounds.," *Journal of cutaneous medicine and surgery*, Vol. 3, pp. S1–1, 1998.

58. Vanwijck, R., "Surgical biology of wound healing," *Bulletin et memoires de l'Academie royale de medecine de Belgique*, Vol. 156, no. 3-4, pp. 175–84, 2000.

59. Suan, L. P., N. Bidin, C. J. Cherng, and A. Hamid, "Light-based therapy on wound healing: a review," *Laser Physics*, Vol. 24, no. 8, p. 083001, 2014.

60. Chaves, M. E. d. A., A. R. d. Araújo, A. C. C. Piancastelli, and M. Pinotti, "Effects of low-power light therapy on wound healing: Laser x led," *Anais brasileiros de dermatologia*, Vol. 89, no. 4, pp. 616–623, 2014.

61. Kanitakis, J., "Anatomy, histology and immunohistochemistry of normal human skin.," *European journal of dermatology: EJD*, Vol. 12, no. 4, pp. 390–9, 2001.

62. Birgersson, U., *Electrical impedance of human skin and tissue alterations: Mathematical modeling and measurements*, Inst för klinisk vetenskap, intervention och teknik/Dept of Clinical Science, Intervention and Technology, 2012.

63. Nielsen, K. P., L. Zhao, J. J. Stamnes, K. Stamnes, and J. Moan, "The optics of human skin: Aspects important for human health," *Nor. Acad. Sci. Lett*, Vol. 2008, pp. 35–46, 2008.

64. Jacques, S. L., and D. J. McAuliffe, "The melanosome: threshold temperature for explosive vaporization and internal absorption coefficient during pulsed laser irradiation," *Photochemistry and photobiology*, Vol. 53, no. 6, pp. 769–775, 1991.

65. Prahl, S., *et al.*, "Optical absorption of hemoglobin," *Oregon Medical Laser Center, http://omlc. ogi. edu/spectra/hemoglobin/index. html*, Vol. 15, 1999.

66. Bendit, E., and D. Ross, "A technique for obtaining the ultraviolet absorption spectrum of solid keratin," *Applied Spectroscopy*, Vol. 15, no. 4, pp. 103–105, 1961.

67. AlGhamdi, K. M., A. Kumar, and N. A. Moussa, "Low-level laser therapy: a useful technique for enhancing the proliferation of various cultured cells," *Lasers in medical science*, Vol. 27, no. 1, pp. 237–249, 2012.

68. Yu, H.-S., K.-L. Chang, C.-L. Yu, J.-W. Chen, and G.-S. Chen, "Low-energy helium-neon laser irradiation stimulates interleukin-1α and interleukin-8 release from cultured human keratinocytes," *Journal of investigative Dermatology*, Vol. 107, no. 4, pp. 593–596, 1996.

69. Bibikova, A., and U. Oron, "Promotion of muscle regeneration in the toad (bufo viridis) gastrocnemius muscle by low-energy laser irradiation," *The Anatomical Record*, Vol. 235, no. 3, pp. 374–380, 1993.

70. Conlan, M. J., J. W. Rapley, and C. M. Cobb, "Biostimulation of wound healing by low-energy laser irradiation a review," *Journal of clinical periodontology*, Vol. 23, no. 5, pp. 492–496, 1996.

71. Havel, M., C. S. Betz, A. Leunig, and R. Sroka, "Diode laser-induced tissue effects: In vitro tissue model study and in vivo evaluation of wound healing following non-contact application," *Lasers in surgery and medicine*, Vol. 46, no. 6, pp. 449–455, 2014.

72. Hussein, A. J., A. A. Alfars, M. A. Falih, A.-N. A. Hassan, *et al.*, "Effects of a low level laser on the acceleration of wound healing in rabbits," *North American journal of medical sciences*, Vol. 3, no. 4, p. 193, 2011.

73. Basso, F. G., C. F. Oliveira, C. Kurachi, J. Hebling, and C. A. de Souza Costa, "Biostimulatory effect of low-level laser therapy on keratinocytes in vitro," *Lasers in medical science*, Vol. 28, no. 2, pp. 367–374, 2013.

74. Basso, F. G., T. N. Pansani, A. P. S. Turrioni, V. S. Bagnato, J. Hebling, and C. A. de Souza Costa, "In vitro wound healing improvement by low-level laser therapy application in cultured gingival fibroblasts," *International journal of dentistry*, Vol. 2012, 2012.

75. Lane, N., "Cell biology: power games," *Nature*, Vol. 443, no. 7114, pp. 901–903, 2006.

76. Barolet, D., "Light-emitting diodes (leds) in dermatology," in *Seminars in cutaneous medicine and surgery*, Vol. 27, pp. 227–238, Frontline Medical Communications, 2008.

77. Chung, H., T. Dai, S. K. Sharma, Y.-Y. Huang, J. D. Carroll, and M. R. Hamblin, "The nuts and bolts of low-level laser (light) therapy," *Annals of biomedical engineering*, Vol. 40, no. 2, pp. 516–533, 2012.

78. Posten, W., D. A. Wrone, J. S. Dover, K. A. Arndt, S. Silapunt, and M. Alam, "Low-level laser therapy for wound healing: mechanism and efficacy," *Dermatologic surgery*, Vol. 31, no. 3, pp. 334–340, 2005.

79. Kekonen, A., "Bioimpedance measurement device for chronic wound healing monitoring," 2013.

80. Norman K, Stobaus N, Z. D. e. a., "Cutoff percentiles of bioelectrical phase angle predict functionality, quality of life, and mortality in patients with cancer," *Am J Clin Nutr*, Vol. 92, 2010.

81. Paiva, S. I., L. R. Borges, D. Halpern-Silveira, M. C. F. Assunção, A. J. Barros, and M. C. Gonzalez, "Standardized phase angle from bioelectrical impedance analysis as prognostic factor for survival in patients with cancer," *Supportive Care in Cancer*, Vol. 19, no. 2, pp. 187–192, 2011.

82. 82.Pliquett U, P. M., "Impedance spectroscopy for rapid and noninvasive analysis of skin electroporation," *Methods Mol Med.*, Vol. 37, 2000.

83. Osterman, K. S., P. J. Hoopes, C. DeLorenzo, D. J. Gladstone, and K. D. Paulsen, "Non-invasive assessment of radiation injury with electrical impedance spectroscopy," *Physics in Medicine and Biology*, Vol. 49, no. 5, p. 665, 2004.

84. Bauchot, A. D., F. R. Harker, and W. M. Arnold, "The use of electrical impedance spectroscopy to assess the physiological condition of kiwifruit," *Postharvest Biology and technology*, Vol. 18, no. 1, pp. 9–18, 2000.

85. Ulgen, Y., and M. Sezdi, "Hematocrit dependence of the cole-cole parameters of human blood," in *Biomedical Engineering Days, 1998. Proceedings of the 1998 2nd International Conference*, pp. 71–74, IEEE, 1998.

86. Webster, J. G., *Electrical impedance tomography*, Taylor & Francis Group, 1990.

87. Ward, L. C., T. Essex, and B. H. Cornish, "Determination of cole parameters in multiple frequency bioelectrical impedance analysis using only the measurement of impedances," *Physiological measurement*, Vol. 27, no. 9, p. 839, 2006.

88. Sezdi, M., M. Bayik, and Y. Ulgen, "Storage effects on the cole-cole parameters of erythrocyte suspensions," *Physiological measurement*, Vol. 27, no. 7, p. 623, 2006.

89. Palko, T., F. Bialokoz, and J. Weglarz, "Multifrequency device for measurement of the complex electrical bio-impedance-design and application," in *Engineering in Medicine and Biology Society, 1995 and 14th Conference of the Biomedical Engineering Society of India. An International Meeting, Proceedings of the First Regional Conference., IEEE*, pp. 1–45, IEEE, 1995.

90. Steendijk, P., G. Mur, E. T. Van Der Velde, and J. Baan, "The four-electrode resistivity technique in anisotropic media: theoretical analysis and application on myocardial tissue in vivo," *IEEE Transactions on Biomedical Engineering*, Vol. 40, no. 11, pp. 1138–1148, 1993.

91. Boulton, M., and J. Marshall, "He-ne laser stimulation of human fibroblast proliferation and attachment in vitro," *Lasers in the life sciences*, Vol. 1, no. 2, pp. 125–134, 1986.

92. Quickenden, T., and L. Danniels, "Attempted biostimulation of division in saccharomyces cerevisiae using red coherent light," *Photochemistry and photobiology*, Vol. 57, no. 2, pp. 272–278, 1993.

93. Schneede, P., W. Jelkmann, U. Schramm, H. Fricke, M. Steinmetz, and A. Hofstetter, "Effects of the helium-neon laser on rat kidney epithelial cells in culture," *Lasers in Medical Science*, Vol. 3, no. 1-4, pp. 249–257, 1988.

94. Hawkins, D., N. Houreld, and H. Abrahamse, "Low level laser therapy (lllt) as an effective therapeutic modality for delayed wound healing," *Annals of the New York Academy of Sciences*, Vol. 1056, no. 1, pp. 486–493, 2005.

95. Lau, P. S., N. Bidin, G. Krishnan, Z. Nassir, and H. Bahktiar, "Biophotonic effect of diode laser irradiance on tensile strength of diabetic rats," *Journal of Cosmetic and Laser Therapy*, Vol. 17, no. 2, pp. 86–89, 2015.

96. Gao, X., and D. Xing, "Molecular mechanisms of cell proliferation induced by low power laser irradiation," *Journal of biomedical science*, Vol. 16, no. 1, p. 1, 2009.

97. Hawkins, D., and H. Abrahamse, "Biological effects of helium-neon laser irradiation on normal and wounded human skin fibroblasts," *Photomedicine and Laser Therapy*, Vol. 23, no. 3, pp. 251–259, 2005.

98. Cristofalo, V. J., C. Volker, and R. G. Allen, "Use of the fibroblast model in the study of cellular senescence," *Aging Methods and Protocols*, pp. 23–52, 2000.

99. Kreisler, M., A. B. Christoffers, H. Al-Haj, B. Willershausen, and B. d'Hoedt, "Low level 809-nm diode laser-induced in vitro stimulation of the proliferation of human gingival fibroblasts," *Lasers in surgery and medicine*, Vol. 30, no. 5, pp. 365–369, 2002.

100. Güngörmüş, M., and U. K. Akyol, "Effect of biostimulation on wound healing in diabetic rats," *Photomedicine and laser surgery*, Vol. 27, no. 4, pp. 607–610, 2009.

101. Riou, J.-P. A., J. R. Cohen, and H. Johnson, "Factors influencing wound dehiscence," *The American journal of surgery*, Vol. 163, no. 3, pp. 324–330, 1992.

102. Santos, N. R., J. N. dos Santos, J. A. dos Reis Jr, P. C. Oliveira, A. P. C. de Sousa, C. M. de Carvalho, L. G. Soares, A. M. Marques, and A. L. B. Pinheiro, "Influence of the use of laser phototherapy (λ660 or 790 nm) on the survival of cutaneous flaps on diabetic rats," *Photomedicine and laser surgery*, Vol. 28, no. 4, pp. 483–488, 2010.

103. Kaviani, A., G. E. Djavid, L. Ataie-Fashtami, M. Fateh, M. Ghodsi, M. Salami, N. Zand, N. Kashef, and B. Larijani, "A randomized clinical trial on the effect of low-level laser therapy on chronic diabetic foot wound healing: a preliminary report," *Photomedicine and Laser Surgery*, Vol. 29, no. 2, pp. 109–114, 2011.

104. Kawalec, J. S., V. J. Hetherington, T. C. Pfennigwerth, D. S. Dockery, and M. Dolce, "Effect of a diode laser on wound healing by using diabetic and nondiabetic mice," *The Journal of foot and ankle surgery*, Vol. 43, no. 4, pp. 214–220, 2004.

105. Stadler, I., R. J. Lanzafame, R. Evans, V. Narayan, B. Dailey, N. Buehner, and J. O. Naim, "830-nm irradiation increases the wound tensile strength in a diabetic murine model," *Lasers in surgery and medicine*, Vol. 28, no. 3, pp. 220–226, 2001.

106. Skopin, M. D., and S. C. Molitor, "Effects of near-infrared laser exposure in a cellular model of wound healing," *Photodermatology, photoimmunology & photomedicine*, Vol. 25, no. 2, pp. 75–80, 2009.

107. Ackmann, J. J., and M. A. Seitz, "Methods of complex impedance measurements in biologic tissue.," *Critical reviews in biomedical engineering*, Vol. 11, no. 4, pp. 281–311, 1983.

108. Martinsen, Ø. G., S. Grimnes, and E. Haug, "Measuring depth depends on frequency in electrical skin impedance measurements," *Skin Research and Technology*, Vol. 5, no. 3, pp. 179–181, 1999.

109. Birgersson, U. H., E. Birgersson, and S. Ollmar, "Estimating electrical properties and the thickness of skin with electrical impedance spectroscopy: Mathematical analysis and measurements," *Journal of Electrical Bioimpedance*, Vol. 3, no. 1, pp. 51–60, 2012.

110. Björklund, S., T. Ruzgas, A. Nowacka, I. Dahi, D. Topgaard, E. Sparr, and J. Engblom, "Skin membrane electrical impedance properties under the influence of a varying water gradient," *Biophysical journal*, Vol. 104, no. 12, pp. 2639–2650, 2013.

111. Spence, D. W., and B. Pomeranz, "Surgical wound healing monitored repeatedly in vivo using electrical resistance of the epidermis," *Physiological measurement*, Vol. 17, no. 2, p. 57, 1996.

112. Keese, C. R., J. Wegener, S. R. Walker, and I. Giaever, "Electrical wound-healing assay for cells in vitro," *Proceedings of the National Academy of Sciences of the United States of America*, Vol. 101, no. 6, pp. 1554–1559, 2004.